

Report no. (NGU): 2004.049		ISSN 0800-3416		Grading: Open	
Report no. (SINTEF): 54.5272.00/02/04					
Title: Storage potential for CO ₂ in the Frohavet Basin, Mid-Norway					
Authors: Szczepan Polak, Erik Lundin, Peter Zweigel, Reidulv Bøe, Erik Lindeberg & Odleiv Olesen			Client: CO2STORE project group		
County: Norway			Commune: Frøya, Hitra, Bjugn, Ørland		
Map-sheet name (M=1:250.000) Trondheim, Kristiansund, Namsos			Map-sheet no. and -name (M=1:50.000) 1422 I (Nord-Frøya), 1422 II (Hitra), 1522 III (Ørland), 1522 IV (Tarva), 1523 III (Halten)		
Deposit name and grid-reference:			Number of pages: 57		Price (NOK): 330,-
Map enclosures:					
Fieldwork carried out:	Date of report: 01.12.2004	Project no.: 299900 (NGU) 54.5272.00(SINTEF)		Person responsible: Terje Thorsnes	
<p>Summary:</p> <p>The sedimentary succession in the subsurface of the Frohavet (Mid-Norway) has been assessed with regard to its suitability for long-term storage of CO₂. This study is part of the EU-funded CO2STORE project and was stimulated by the geographical proximity of the Frohavet Basin to planned CO₂ point sources in Mid Norway.</p> <p>The sedimentary content of the basin has been interpreted based on seismic data, erratic sediment blocks found at the shore in the proximity of the basin, and by analogy to the geology in offshore hydrocarbon fields. The sediments are probably of Jurassic age. Key seismic horizons, including the base of the Quaternary and the top of the basement have been mapped on seismic and depth-converted. Since the basin is nowhere exposed and has not been drilled, the properties of the sedimentary formations are not known. In analogy to the sedimentary succession offshore, two formations with properties suitable for CO₂ injection have been postulated: the 'Ile Formation' and the 'Garn Formation'. Both formations dip to the southeast, and a small anticlinal trap exists at the top of the 'Garn Formation'.</p> <p>A digital subsurface geology model has been generated based on the mapped horizons. Petrophysical properties of the potential reservoir formations are only tentatively known from offshore analogs. Therefore, several cases with variable reservoir properties have been simulated. The simulations assume injection at the base of the deepest postulated reservoir formation.</p> <p>The simulation results show that the basin would not be suitable for long-term CO₂ storage if reservoir permeability is high, if the k_v/k_h ratio is high, or if the relative permeability to gas is high. If, however, these parameters are moderate to low, there may be no leakage for several centuries, and leakage rates afterwards may be acceptable (approximately at, or below 0.01% of the total injected mass). Pore pressure is not expected to increase so much that it would cause fracturing of the overburden. Sensitivity to the governing parameters would require further investigation.</p> <p>The conclusion of this assessment is thus that the Frohavet Basin may be suitable for long-term CO₂ storage given favourable reservoir properties. Further studies should investigate favourable parameter combinations in more detail before acquiring reservoir data from a well.</p>					
Keywords: Aquifer		CO ₂		Carbon dioxide storage	
Reservoir simulation		Numerical modelling		Frohavet	
Leakage rate		Storage capacity		Jurassic	

CONTENTS

- 1. EXECUTIVE SUMMARY 6
- 2. INTRODUCTION..... 9
- 3. GEOLOGY OF THE FROHAVET BASIN 11
 - 3.1 Seismic database 11
 - 3.2 Bathymetry 11
 - 3.3 Quaternary deposits..... 11
 - 3.4 Geometry, sedimentary content, and burial/uplift history..... 13
 - 3.5 Time-depth conversion of seismic data..... 16
 - 3.6 Key features of the Frohavet Basin geology as input to reservoir simulation 19
- 4. RESERVOIR SIMULATION..... 22
 - 4.1 Rationale..... 22
 - 4.2 An outline of major expected processes in the reservoir 22
 - 4.3 Reservoir model and input data..... 23
 - 4.4 Simulation results – predicted leakage rates 33
 - 4.4.1 Base case 33
 - 4.4.2 Alternative cases 38
 - 4.5 Simulation results - pressure development..... 48
- 5. DISCUSSION AND CONCLUSIONS..... 51
- 6. ACKNOWLEDGEMENTS 54
- 7. REFERENCES 55

FIGURES

Figure 1.1 Cross section through the Frohavet Basin. Upper: Seismic section with main seismic units. Lower: representation in the geological model and terminology in analogy to the offshore area.

Figure 2.1 Geological map of Mid-Norway showing the main structural provinces. The location of Skogn and of the Frohavet Basin are shown. Modified from Blystad et al. (1995).

Figure 3.1 Seismic grid, Frohavet. The Jurassic Frohavet Basin is shown in blue. Modified from Sommaruga & Bøe (2002).

Figure 3.2 Bathymetry of Frohavet. The digital map is based on the bathymetric map in Bøe (1991).

Figure 3.3 Geological map of the Frohavet Basin. See Figure 3.4 for colour legend. Modified from Sommaruga & Bøe (2002).

Figure 3.4 Interpreted seismic line across Frohavet. Note that the Jurassic sedimentary succession is downthrown in the southeast along the Tarva Fault. See Figure 3.1 for location of the seismic profile. Modified from Sommaruga & Bøe (2002).

Figure 3.5 Depth (m) to top basement below the Jurassic Frohavet Basin.

Figure 3.6 Depth (m) to top Unit C, Frohavet Basin.

Figure 3.7 Depth (m) to top Unit B, Frohavet Basin.

Figure 3.8 Thin section of sandstone from an erratic boulder found on the Froan Islands. Note the high degree of cementation and patchy porosity (8%, mainly dissolution porosity). Sample 82-87. Picture: Mai Britt Mørk.

Figure 4.1 Cross-sections through the reservoir model of the Frohavet Basin (for location see Figure 4.2). The formation colour code is identical in the two cross-sections. The single-layer model representation of seawater is shown as a dark blue layer above the thin (light blue) Quaternary.

Figure 4.2 Depth to the top 'Garn' Formation. Red lines indicate cross sections (Figure 4.1) and arrows denote injection points used in simulations. Injection point 1 is the base case location.

Figure 4.3 Depth map of the base of the 'Melke' Formation indicating a dipping anticline which serves as a trap in several simulations.

Figure 4.4 Calculated temperature, pore pressure and pT-dependent CO₂ density versus depth for the Frohavet Basin.

Figure 4.5 CO₂ density vs. pressure at reservoir temperature of 29°C.

Figure 4.6 CO₂ viscosity vs. pressure at reservoir temperature of 29°C

Figure 4.7 Density of reservoir water at different CO₂ saturation vs. pressure at reservoir temperature of 29°C

Figure 4.8 Viscosity of reservoir water at different CO₂ saturation vs. pressure at reservoir temperature of 29°C

Figure 4.9 Relative permeability curves used for water and CO₂ in the water-CO₂ system

Figure 4.10 Simulated fraction of total injected CO₂ predicted to have leaked from the reservoir for the base case.

Figure 4.11 Gas saturation in the reservoir after 25 years of CO₂ injection. NW is left.

Figure 4.12 Gas saturation at the top of the 'Garn' Formation after 25 years (upper left), 100 years (upper right) and 2000 years (lower).

Figure 4.13 Simulated fraction of total injected CO₂ predicted to have leaked from the reservoir; effect of changes to the absolute permeability, porosity and k_v/k_h ratio

Figure 4.14 Simulated fraction of total injected CO₂ predicted to have leaked from the reservoir; effect of different location of injection points and effect of number of injection wells. Both curves: $k_h = 20$ mD, poro = 12.5%, $k_v/k_h = 0.1$.

Figure 4.15 Base case and alternative relative permeability curves used for water and CO₂ in the water-CO₂ system. For parameters see Table 4.6.

Figure 4.16 Capillary pressure curve for irreducible water saturation of $S_{wr}=0.11$. For parameters see Table 4.6.

Figure 4.17 Simulated fraction of total injected CO₂ predicted to have leaked from the reservoir; effect of use of alternative relative permeability curves and of dependency of gas and water saturation on capillary pressure ('with Pc', versus 'no Pc')

Figure 4.18 Simulated fraction of total injected CO₂ predicted to have leaked from the reservoir; effect of low permeability in the 'Garn' Formation

Figure 4.19 CO₂ saturation at the top of the 'Garn' Formation after 200 years (left) and 2000 years (right); case with reduced permeability of the 'Garn' Formation.

Figure 4.20 Pressure development below the 'Melke' Formation for three selected cases..

TABLES

Table 3.1 Velocities used to depth convert the time structure map.

Table 4.1 Seismic units, formations, and their status in simulations

Table 4.2 Construction parameters for cells in the modelled formations in the subsurface geology model (Irap RMS).

Table 4.3 Reservoir parameter range applied to the formations in the Frohavet Basin

Table 4.4 Calculated reservoir volumes (in Eclipse) in 10^6 m³

Table 4.5 Parameters used for simulation in the base case.

Table 4.6 Parameters used in calculation of alternative relative permeability curves and a capillary pressure curve.

1. EXECUTIVE SUMMARY

Plans for a combined heat and power plant (CHP) in Skogn in the inner part of the Trondheimsfjord (Mid-Norway) include options to capture CO₂ from the flue gas stream. At Tjeldbergodden in Mid-Norway, a methanol plant emits at present approximately 450 000 tonnes of CO₂ per year, and plans exist to build an additional methanol plant there with a similar CO₂ emission and a gas-fired power plant which would emit approximately 2 100 000 tonnes of CO₂ per year. In order to reduce anthropogenic greenhouse gas emissions, several potential sites for underground storage of CO₂ are investigated as part of the EU- and industry-funded project CO₂STORE. One of the potential storage sites in Mid-Norway is the Frohavet Basin. The Beitstadfjord Basin close to the CHP in Skogn has been assessed in an earlier study (Polak et al 2004) which concluded that that basin was not suitable for long-term CO₂ storage. This report documents the results of an assessment of the subsurface sedimentary succession of the Frohavet Basin with regard to its suitability for long-term storage of CO₂.

The objective of the assessment is to predict if CO₂ injected at the typical emission rate from a CHP of approximately 2 000 000 tonnes per year would stay in the subsurface and would leak - if at all - at a rate acceptable to reach long-term goals for maximum atmospheric CO₂ concentrations.

The geometry and sedimentary content of the basin have been interpreted from seismic data. The basin forms a half-graben with a major normal fault at its southeastern margin. Four main sedimentary units have been distinguished, three of which (named seismic units A, B, and C) dip towards the southeast (Figure 1.1). The Quaternary, as the fourth sedimentary unit, overlies the other formations discordantly. It has a thickness of locally up to approximately 75 m, but is mostly much thinner and is most probably locally absent.

The basin has not been drilled and information about the age and lithology of the three pre-Quaternary units has therefore been derived from blocks found at the shores of the surrounding of the basin. These blocks indicate a Middle Jurassic age. The three units have tentatively been correlated to formations known from numerous wells in the offshore hydrocarbon province of the Halten Terrace, among them two formations with possibly favourable reservoir properties: the 'Ile' and 'Garn' formations. According to the seismic data, these formations constitute in the Frohavet Basin largely an open, dipping reservoir. A minor dipping anticlinal trap exists at the top of the 'Garn' Formation.

A digital subsurface geology model has been generated based on the mapped horizons. Since the petrophysical properties of the potential reservoir formations are not known due to the lack of wellbore data, they had to be estimated based on the offshore geological analogs. The implicit uncertainty was addressed by simulation of a range of cases with varying reservoir properties (porosity, horizontal permeability, k_v/k_h ratio, relative permeability, residual gas saturation, fluid saturation dependence on capillary pressure).

At the probable pressure and temperature conditions in the Frohavet Basin, CO₂ will have a relatively high density of approximately 800 kg/m³ below a depth of about 450 m bsl. This is lower than the density of the formation water. The main process expected to occur in case of CO₂-injection into the Frohavet Basin is buoyancy-driven upward migration until the CO₂ reaches an impermeable formation (the 'Melke' Formation). It will fill available traps at this level and then migrate upwards along the top of the reservoir formation until it escapes into

the sea water in the Frohavet. Some CO₂ will be trapped in the pore space as residual gas. Some additional CO₂ will be dissolved into formation water in the reservoir unit, but this process is slow, operating over a time scale of 1000s of years.

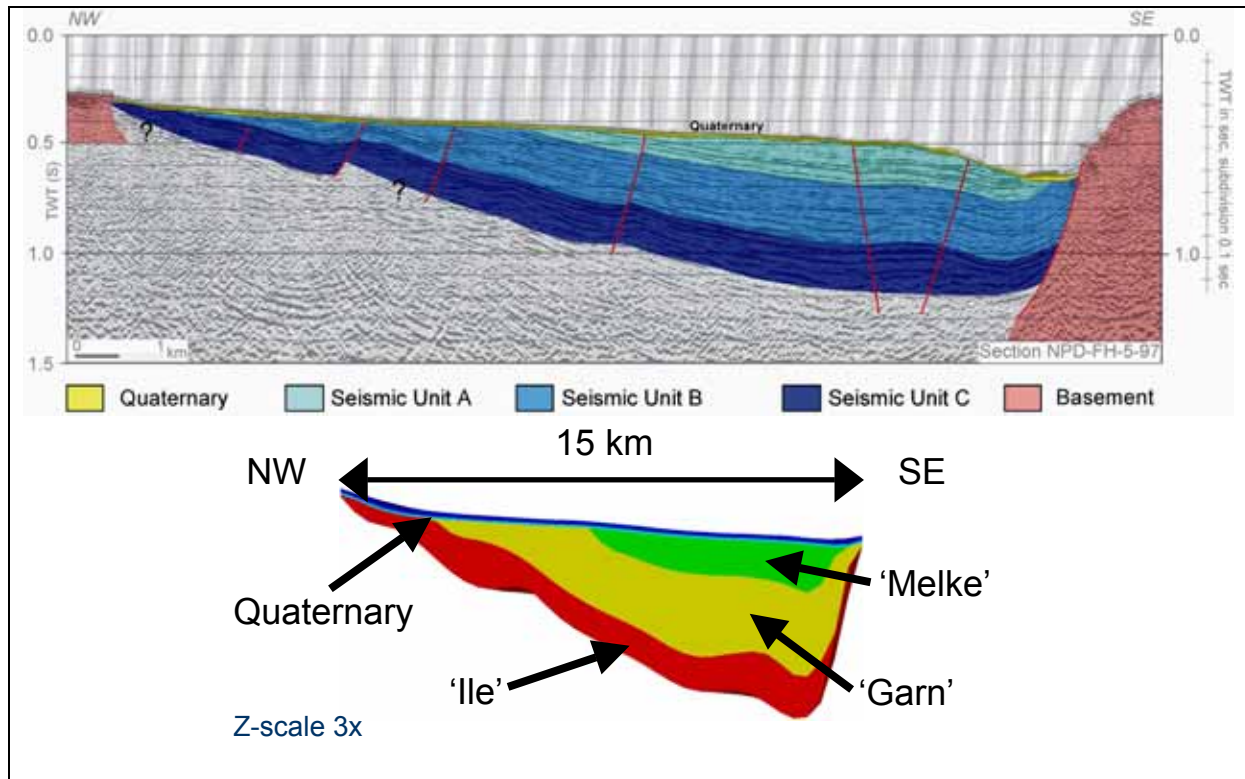


Figure 1.1 Cross section through the Frohavet Basin. Upper: Seismic section with main seismic units. Lower: representation in the geological model and terminology in analogy to the offshore area.

If formation water and CO₂ can leave the storage reservoir only at a very low rate, pore pressure in the reservoir will increase. This pore pressure increase may induce hydraulic fracturing of the seal, generating highly efficient pathways for pressure release and migration of CO₂ from the reservoir unit into the sea water. It is estimated that in the Frohavet case a pore pressure increase in the reservoir of more than 13.6 bars may cause hydraulic fracturing of the seal. However, such an overpressure is unlikely to occur according to the simulations reported here, because the site is an open system (the Quaternary is not sealing) and because the accessible pore volume in the basin is large.

Reservoir simulations were carried out to test if CO₂ injected at a rate of 2 million tonnes per year would leak from the reservoir. The simulations assume injection close to the base of the deepest of the two reservoir formations.

The simulations predict early leakage and unacceptably high leakage rates in the case of high absolute permeability (2000 mD), high k_v/k_h ratio (1/10), and high relative permeability to gas. In the worst case (the ‘base case’), leakage is predicted to start 10 years after injection start and cumulative leakage is predicted to be 86% of the injected quantity at 50 years after injection start.

However, if these parameters are moderate to low, there may be no leakage for several centuries, and leakage rates afterwards may be acceptable (annual leakage rate at approximately or below 0.01% of the total injected mass).

Sensitivity of the simulation results to some of the governing parameters could not be fully studied within the frame of the project. Further work is required especially to investigate which parameter combinations would be reasonable. In addition, simulated 'safe' storage as residual gas in pores should be analysed in more detail, because this process may have been overestimated due to upscaling procedures.

The conclusion of this assessment is thus that the Frohavet Basin may be suitable for long-term CO₂ storage given favourable reservoir properties. Further studies should investigate favourable parameter combinations in more detail before acquiring reservoir data from a well.

2. INTRODUCTION

Industrikraft Midt-Norge (IMN) is planning to build a combined heat and power plant (CHP) at Fiborgtangen in Skogn (Figure 2.1) in the inner part of Trondheimsfjorden. The plant shall utilize natural gas from Haltenbanken, off Mid-Norway. At Tjeldbergodden in Mid-Norway (Figure 2.1), a methanol plant emits at present approximately 450 000 tonnes of CO₂ per year, and plans exist to build an additional methanol plant there with a similar CO₂ emission and a gas-fired power plant which would emit approximately 2 100 000 tonnes of CO₂ per year. In the EU-funded GESTCO-project, the total storage capacity for CO₂ in aquifers offshore Mid-Norway was estimated to be ca. 30 000 Mt, assuming a storage efficiency of 2% for the aquifers (Bøe et al. 2002). A significant portion of this storage capacity is on the southeastern part of the Trøndelag Platform (east and south of the major hydrocarbon province on the Halten Terrace/Nordland Ridge). It was also mentioned (Bøe et al. 2002) that Frohavet and Beitstadfjorden could have storage potential for CO₂. CO₂ storage in oil and gas fields on the Halten Terrace will not be possible in the next ten to twenty years (except for enhanced oil recovery) due to probable conflicts with the hydrocarbon exploitation. The alternative is thus to store CO₂ in aquifers east and south of the major hydrocarbon province, an area which has previously not been mapped in detail for the purpose of CO₂ storage. This area has the advantage of being closer to onshore CO₂ point sources, which will require shorter pipelines.

With this background, it was decided to participate in the partly EU-funded project CO2STORE, which runs from 2003 to 2005 and which aims to prepare the ground for widespread underground storage of CO₂. The project shall investigate how lessons learned from previous projects, e.g. SACS, GESTCO and NASCENT, can be implemented for CO₂ storage in European aquifers offshore and on land. The project is organized in the following four work packages:

- WP1, Transfer of technology to four other potential demonstration projects (Feasibility Case Studies).
- WP2, Long-term behaviour of injected CO₂
- WP3, Monitoring
- WP4, Management

As part of WP1, a 'Feasibility Case Study Mid-Norway' is carried out in cooperation between the Geological Survey of Norway (NGU), SINTEF Petroleum Research, Industrikraft Midt-Norge (IMN) and Statoil. The objectives of this feasibility case study are to:

- Identify suitable saline aquifers for underground CO₂ storage on the southeastern part of the Trøndelag Platform and in fjords along the coast of Mid-Norway.
- Determine storage capacity by regional mapping, reservoir parameter quantification, and simulation of migration and underground behaviour of CO₂ in these aquifers.
- Investigate and evaluate stability of CO₂ storage in the study area. The risk for, mechanism behind and effect of potential leakages from the storage formations will be studied.
- Suggest further investigations of prospective aquifers.

In this report, the results of the mapping, reservoir parameter quantification and migration simulation for the Frohavet Basin are summarized, and the storage capacity is evaluated.

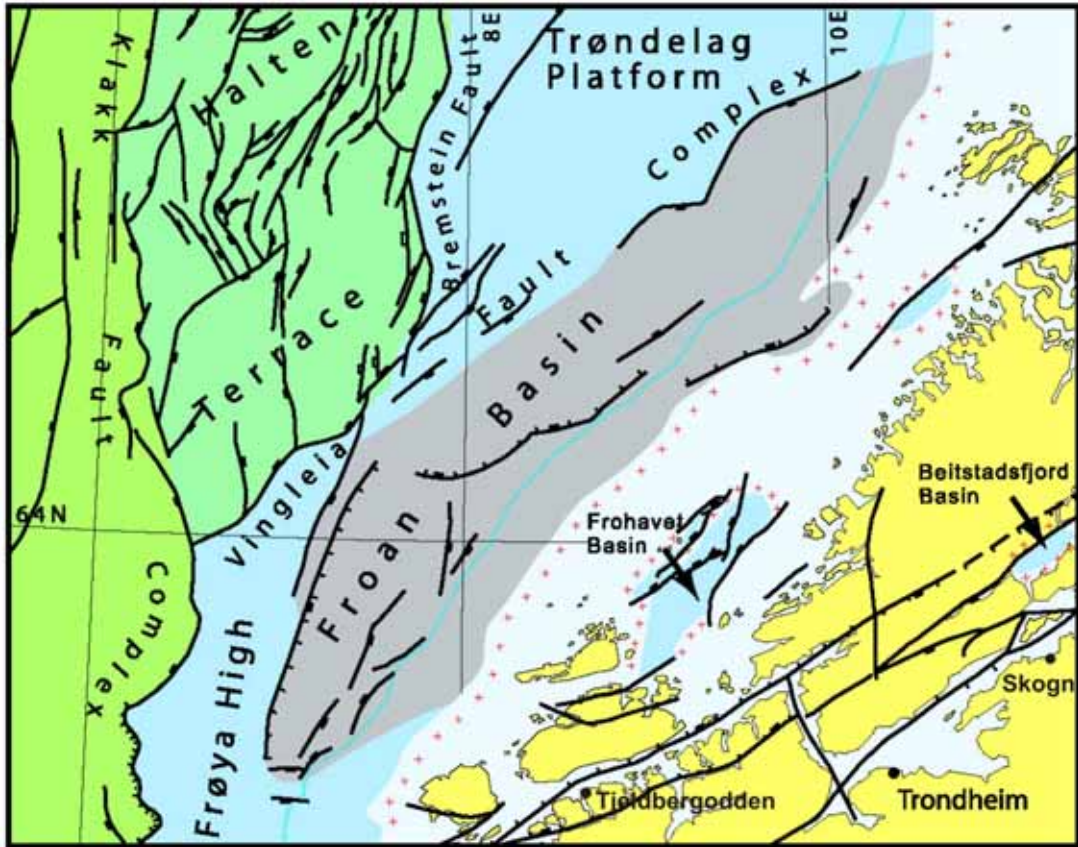


Figure 2.1 Geological map of Mid-Norway showing the main structural provinces. The locations of Skogn, Tjeldbergodden and of the Frohavet Basin are shown. Modified from Blystad et al. (1995).

3. GEOLOGY OF THE FROHAVET BASIN

3.1 Seismic database

The Frohavet Basin is sparsely covered by 2D multichannel seismic data. Four seismic profiles, totalling ca. 100 km in length, were acquired as part of the Kyst-97 survey by the Norwegian Petroleum Directorate. In addition, NGU has acquired 750 km single channel seismic profiles in the Frohavet Basin (Figure 3.1, Bøe 1991, Sommaruga & Bøe 2002). The Kyst-97 data penetrates the entire sedimentary succession, while the NGU data only image the upper 0.350 s TWT (seconds two-way travel time). In this project, the four Kyst-97 profiles were primarily used for mapping since they image the entire sedimentary sequence. The NGU profiles were used as complementary data to define the basin outline and to estimate the trend of the basin dip in the shallowest portion.

3.2 Bathymetry

Frohavet reaches a water depth of more than 500 m in its southeastern part (Figure 3.2). The depth is greatest along a 20-km stretch north and northeast of the Tarva Island, along the trace of the Tarva Fault. There is a gradual decrease in water depth towards the west and northwest. Water depths are everywhere more than 200 m above the part of the Frohavet Basin that is considered for CO₂ storage (see below).

3.3 Quaternary deposits

The Quaternary succession in Frohavet is generally less than 10 m thick (in some areas close to zero) and dominated by hemipelagic silty clays post-dating the last glaciation of the area (Bøe 1991). Only in topographic depressions southeast of the Froan islands, locally along the traces of the Tarva and Dolmsundet Faults, and in an area north of Ulvøya there are Quaternary deposits (units of till and silty clay) up to 75 m thick. Middle Jurassic erratic blocks are found in beach deposits on the Froan islands. These were eroded from the Jurassic Frohavet Basin and deposited by ice streams moving towards the northwest during the final stages of the last glaciation.

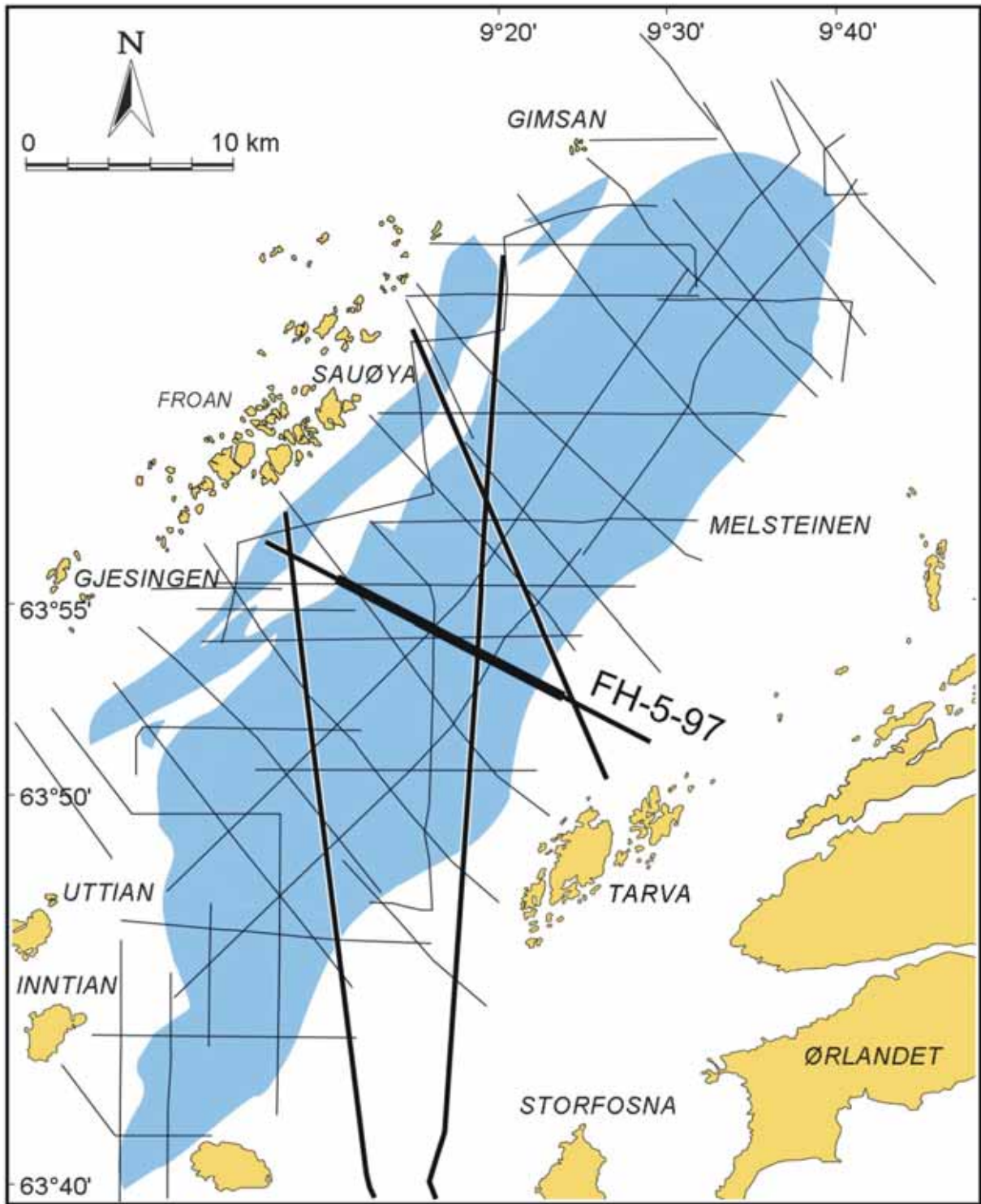


Figure 3.1 Seismic grid, Frohavet. The Jurassic Frohavet Basin is shown in blue. Modified from Sommaruga & Bøe (2002).

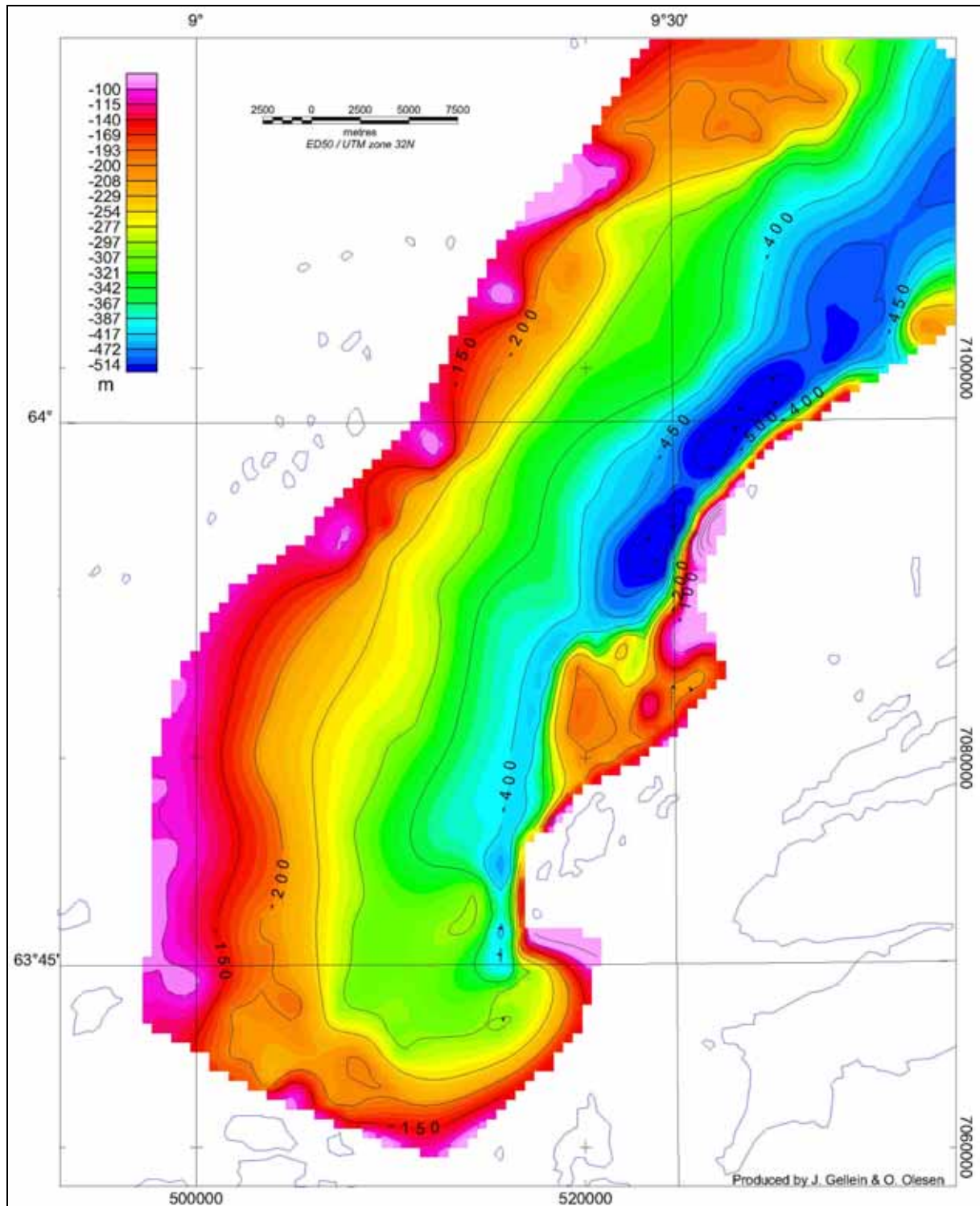


Figure 3.2 Bathymetry of Frohavet. The digital map is based on the bathymetric map in Bøe (1991).

3.4 Geometry, sedimentary content, and burial/uplift history

The Frohavet Basin, which contains a sedimentary rock succession of Middle Jurassic age, is an approximately 60 km long by 15 km wide half graben located northeast of Frøya, on the

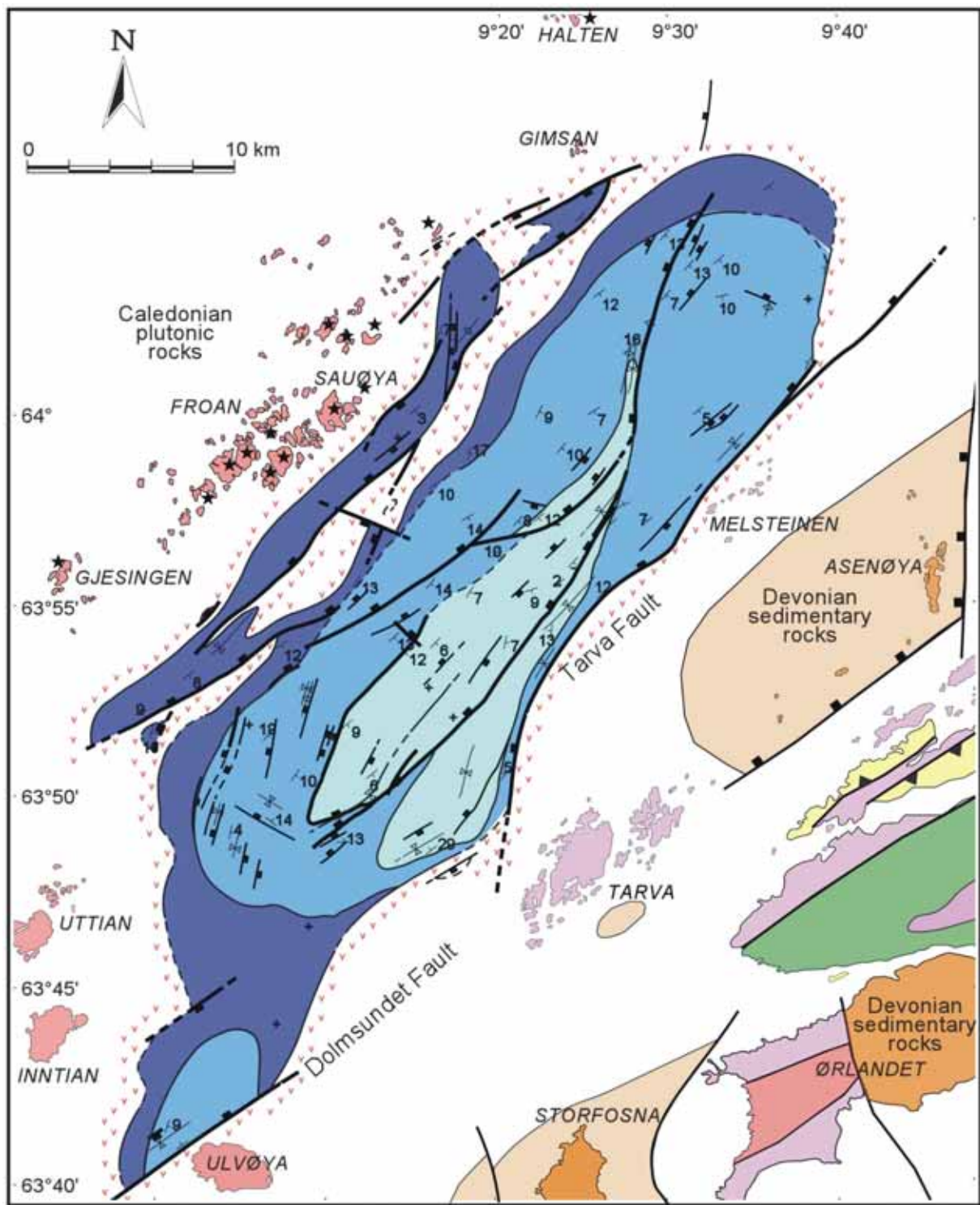
inner part of the Trøndelag Platform (Figure 3.3, Oftedahl 1975, Bøe 1991, Sommaruga & Bøe 2002). The Frohavet Basin borders the Møre-Trøndelag Fault Complex (MTFC), which is a major Caledonian strike-slip structure that has experienced several phases of movement between Devonian and Tertiary time (Gabrielsen et al. 1999). The basin is surrounded by Caledonian plutonic rocks to the northwest, west and southwest. Southeast of the basin, the bedrock is dominated by various gneisses overlain by Devonian sedimentary rocks (Figure 3.3). The Devonian rocks, which are very low grade metamorphosed and with practically zero porosity and permeability, may also be present below the Jurassic succession in Frohavet (Bøe 1991).

The NE-trending half graben dips to the SE, against the Tarva and Dolmsundet normal faults (Figure 3.4). To the southwest, northwest and northeast, the Jurassic rocks lie unconformably on basement. The sedimentary succession in the Frohavet Basin displays a weak expansion towards the bounding faults, i.e. indicating syndepositional growth. Between the main Frohavet basin and the Froan islands, several smaller, fault-bounded basins with Jurassic sedimentary rocks occur (Figure 3.3). The effect of the uniformly SE-dipping bedding is that closure depends on the seal of overlying sediments. The thin cover of Quaternary moraine and clays cannot be expected to provide a top seal for injected CO₂.

There is no well control in the Frohavet Basin. Besides seismic character, the age and type of basin fill have been assessed from loose blocks, plucked by the glaciers and deposited to the northwest on the Froan Islands (Nordhagen 1921, Oftedal 1975, Johansen et al. 1988, Rise et al. 1989). The erratic blocks are made up of various marine and nearshore, fine- to coarse-grained sandstones, conglomerates and mudstones. The blocks are usually cemented by carbonate, and siderite cement is common, especially in the mudstones. The blocks frequently contain coal fragments and shells. In contrast to Beitstadfjorden, the Frohavet samples do not contain freshwater fossils. In an unpublished biostratigraphic analysis of erratic blocks from the Frohavet Basin, Kelly (1988) concluded that the sediments were deposited in Late Bathonian to Early Callovian time. The marine fauna has a Boreal affinity, i.e. indicating that the marine seaway was connected with the Arctic. Kelly (1988) proposed that the sideritic mudstones formed during an earlier Middle Jurassic regression, while the marine sandstones were laid down during a later Middle Jurassic transgression.

The same stratigraphic subdivision has been suggested for the Frohavet Basin as for the Beitstadfjorden Basin (Bøe & Bjerkli 1989, Bøe 1991, Sommaruga & Bøe 2003), which in both cases is based on seismic character and age and lithology of erratic blocks. The sedimentary succession has been divided into Units A-C, that are proposed to be correlative with the Middle Jurassic Melke, Garn and Ile Formations known offshore mid-Norway.

The basin is relatively shallow, with a maximum depth of ca. 1.2 s TWT (ca. 1.6 km, see chapter 3.5). It is clear that the basin has been uplifted and significantly eroded (see chapter 3.6). Evidence for the uplift is provided by: a) seismic velocities (Oftedahl 1975) that are too high for the current basin depth, b) truncation of the dipping Middle Jurassic beds below the Quaternary unconformity, and c) diagenetic studies.



Structural data modified from Bøe (1991)

Figure 3.3 Geological map of the Frohavet Basin. See Figure 3.4 for colour legend. Modified from Sommaruga & Bøe (2002).

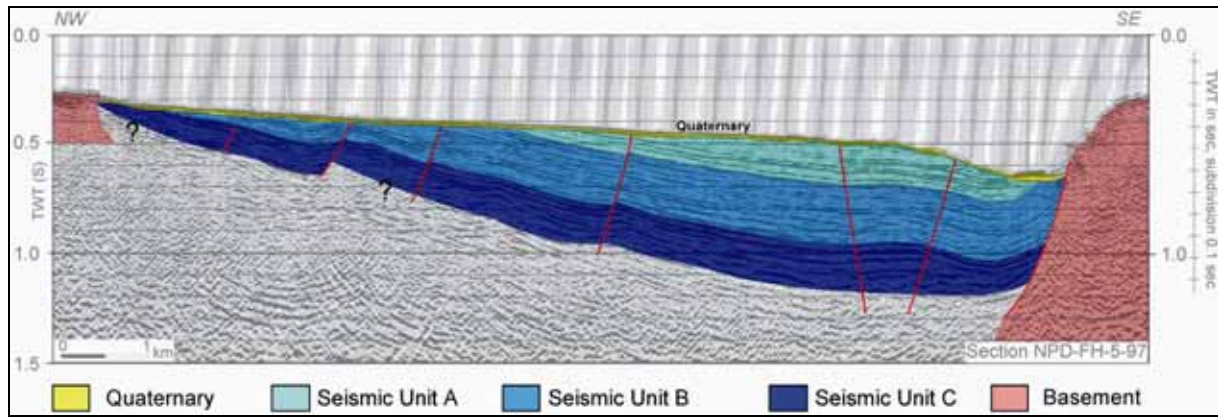


Figure 3.4 Interpreted seismic line across Frohavet. Note that the Jurassic sedimentary succession is downthrown in the southeast along the Tarva Fault. See Figure 3.1 for location of the seismic profile. Modified from Sommaruga & Bøe (2002).

3.5 Time-depth conversion of seismic data

Depth converted time structure maps of top basement, top Unit C and top Unit B are shown in Figure 3.5, Figure 3.6 and Figure 3.7. The velocity for the fine-grained Quaternary sediments is assumed to be around 1.6 km/s. The Quaternary deposits are generally thin and in many cases below the resolution of the seismic data. The Quaternary deposits have therefore not been considered in the depth conversion. The velocity of the Jurassic succession is based on refraction velocities from the Beitstadjord Basin (Oftedal 1975) and common refraction velocities for the Middle Jurassic in the Haltenbanken area.

Table 3.1 Velocities used to depth convert the time structure map.

Interval	Velocity
Sea water	1.48 km/s
Jurassic sedimentary rocks	3.6 km/s

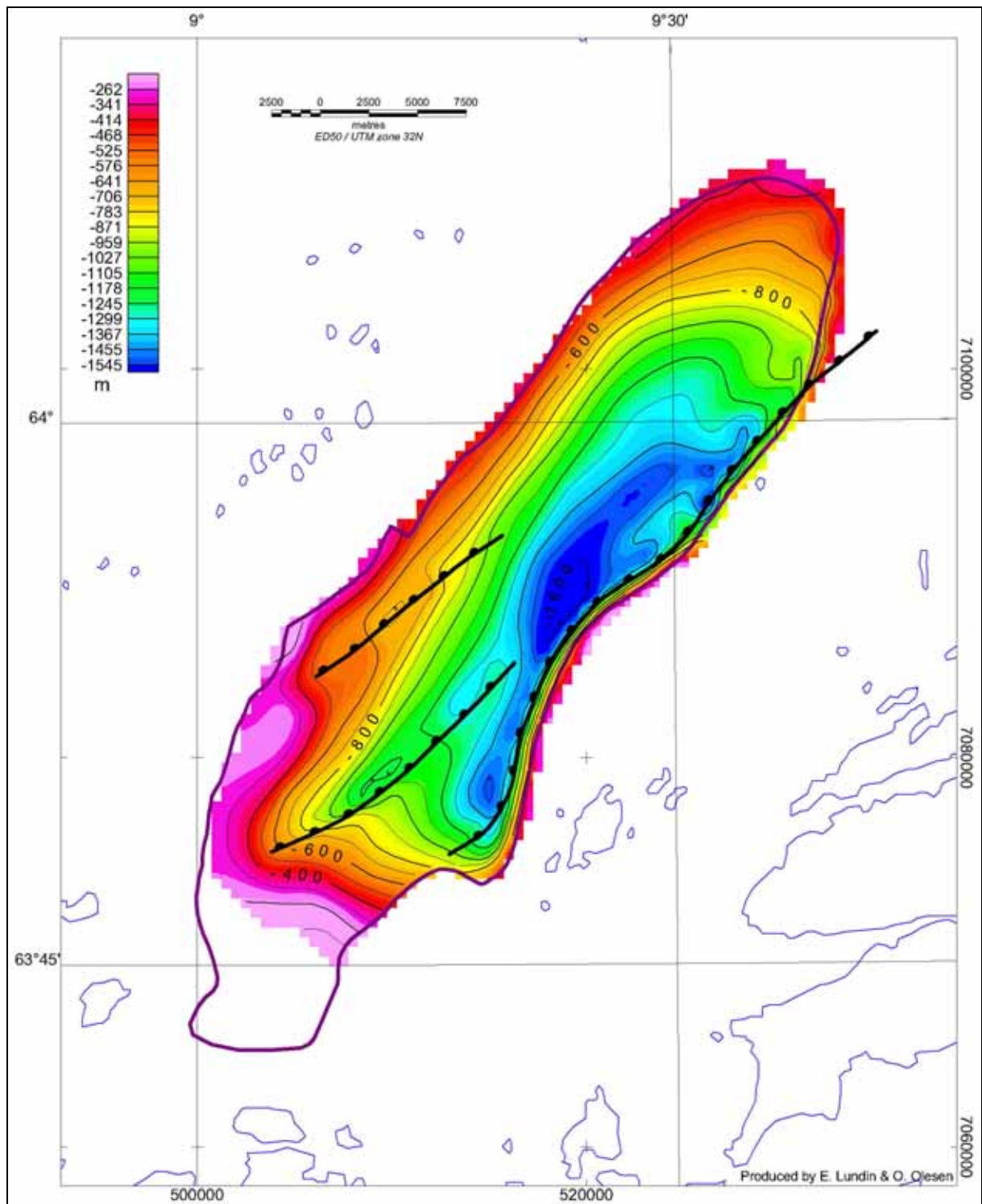


Figure 3.5 Depth (m) to top basement below the Jurassic Frohavet Basin.

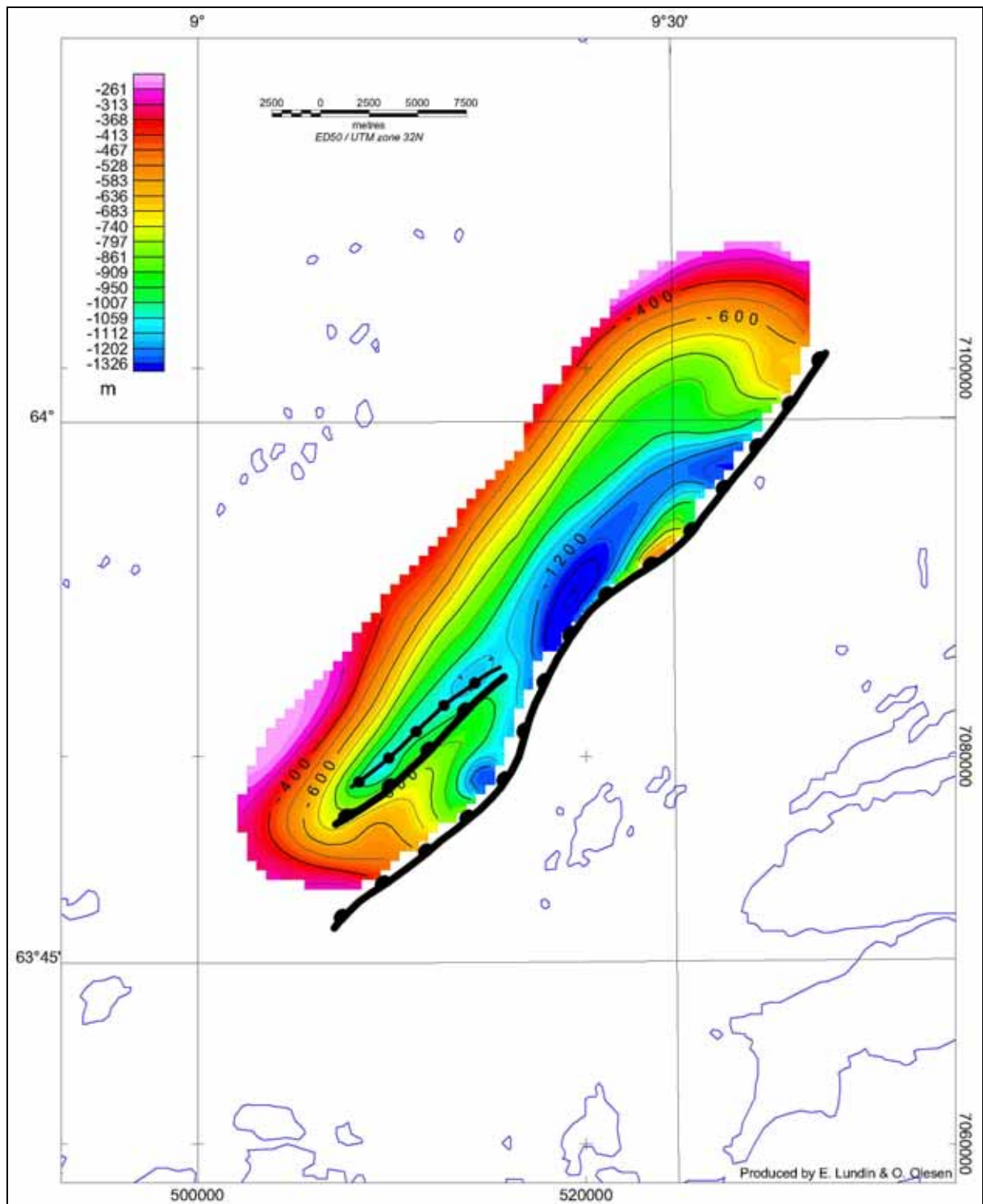


Figure 3.6 Depth (m) to the base of Unit B, Frohavet Basin.

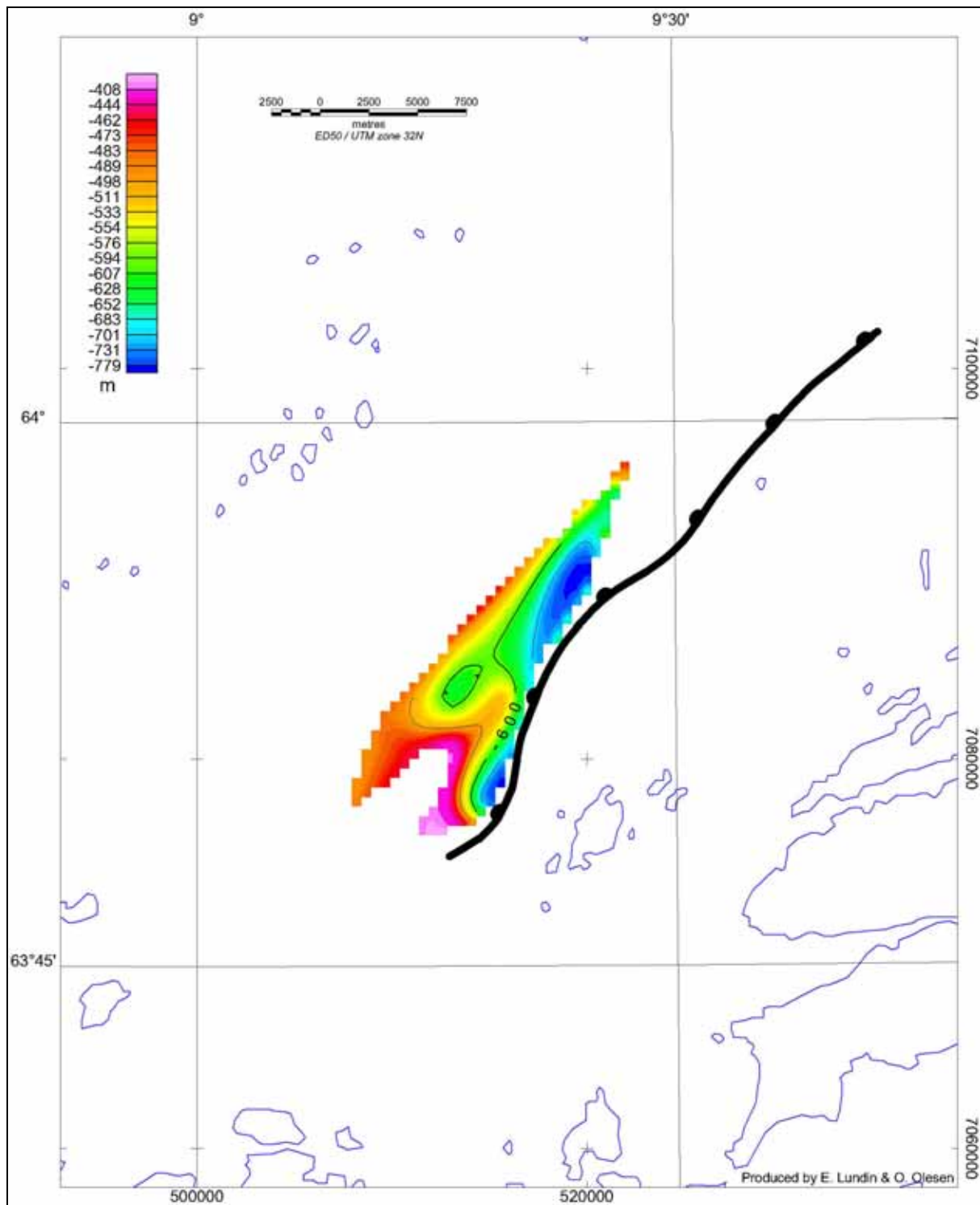


Figure 3.7 Depth (m) to the base of Unit A, Frohavet Basin.

3.6 Key features of the Frohavet Basin geology as input to reservoir simulation

The Frohavet Basin is characterized by a simple geometry, homoclinally dipping to the southeast. Although some minor faults do exist within the basin, these are not considered to be large enough to generate significant independent traps. With the present poor knowledge of the basin stratigraphy, it appears inappropriate to include possible fault barriers in a model.

Thus, for the modelling purposes, the basin is treated as a simple SE-dipping homocline. The basin subcrops below a very thin Quaternary cover, which is not considered to be an efficient top seal.

There are no published seismic refraction velocities for the Frohavet Basin. A study of organic matter maturation gave poor results (Gran 1990). But, based on diagenesis, Gran (1990) estimated a maximum burial temperature between 50°C and 70°C for the sedimentary rock fragments plucked from the seafloor in Frohavet. With a geothermal gradient of ca. 30°C/km, this implies a maximum burial depth of 1.7-2.3 km. The Frohavet Basin lies closer to the hingeline between net uplift and net subsidence (Riis 1996) than the Beitstadvjord (Polak et al. 2004). According to the regional assessment by Riis (1996), the Frohavet area has experienced approximately 500 m of Neogene uplift. The latter estimate needs not be inconsistent with the previous since more than one post-Jurassic uplift may have taken place.

For the purpose of modelling fluid flow in the basin, aquifer properties have been estimated from the estimated maximum burial depth. If we assume a maximum burial depth of 1.7 km for the shallowest part of the basin (which is a minimum estimate according to Gran (1990)), but higher than the Neogene estimate of 750 m of Riis (1996), the maximum burial depth for the deepest part will be ca 2.8 km. These numbers are in accordance with calculated values for maximum burial depth of Jurassic sediments in Beitstadvjorden (Weisz 1992, Polak et al. 2004).

The porosity of the erratic sandstone blocks is poor (generally less than 8%) due to significant cementation (Figure 3.8, Johansen et al. 1988, Mørk et al. 2003). However, it is likely that these blocks are unrepresentative of the succession as a whole since they likely are preferentially preserved due to their resistance to erosion. The preserved blocks are thought to represent highly cemented layers, carbonate concretions in sandstone and sideritic concretions in mudstone. Medium to coarse grained sandstones from erratic blocks have yielded estimated original porosities of 35% and 32 % respectively (Gran 1990). These values are not the actual present day porosity, but the porosity prior to cementation. Gran (1990) concluded that cementation occurred early, prior to mechanical compaction. Mørk et al. (2003) have estimated that the porosity in non-cemented sandstone beds may be 10-20%, even at the present burial depths. From petrography they conclude that the sandstones are mineralogically immature and relatively rich in Fe- and Ca-minerals which can react with CO₂ to form carbonate minerals. The main challenge is to be able to predict the distribution of the carbonate cemented and porous intervals at depths, which will require drilling throughout the succession.

We have too little stratigraphic information to subdivide the basin fill into sandstone versus shale sequences. Lacking knowledge of the actual stratigraphy, a hypothetical aquifer has been placed directly over basement. In doing so, one achieves an optimistic position of an aquifer, since deposition of CO₂ should be performed at a depth of at least ca. 800 m. Suggesting a much shallower aquifer would immediately rule out the basin as a possible storage site for CO₂, making modelling redundant. The thickness of the aquifer is unknown, and cannot be assessed from the seismic data. If the deepest possible aquifer is shown to be unsuitable after the modelling is performed, one can rule out the basin as a potential storage site for CO₂. Should the modelling yield an acceptable result, actual stratigraphy and aquifer properties should be established by stratigraphic drilling.

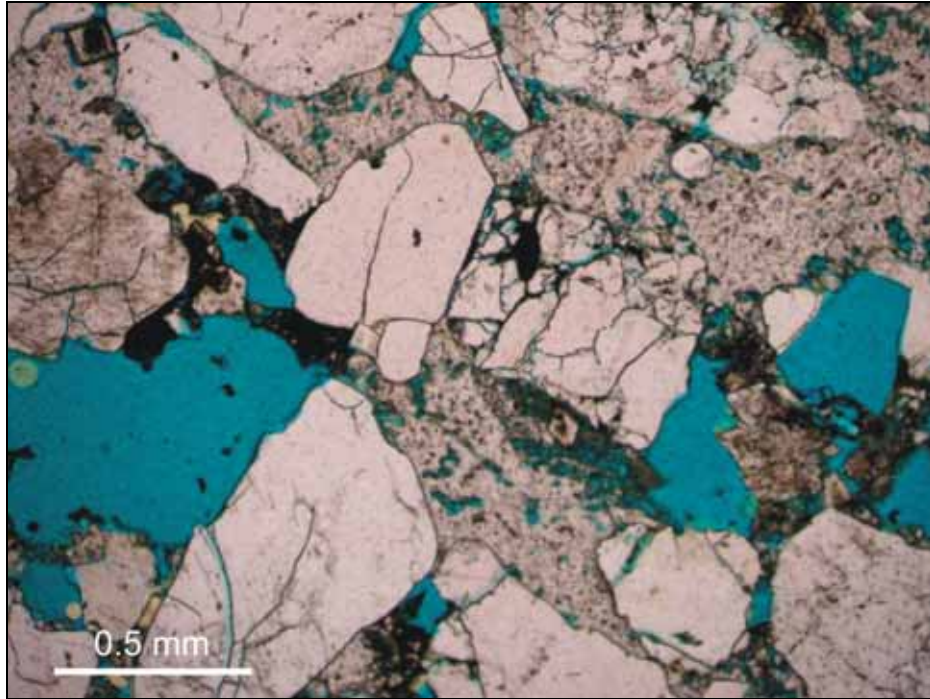


Figure 3.8 Thin section of sandstone from an erratic boulder found on the Froan Islands. Note the high degree of cementation and patchy porosity (8%, mainly dissolution porosity). Sample 82-87. Picture: Mai Britt Mørk.

The nearest shallow IKU stratigraphic wells that have drilled Jurassic sequences are those belonging to the B85 sampling program, located ca 100 km northwest of the basin. These samples were collected with electric rock core drilling and vibrocore, which limited the core lengths to 5.5 m and 6 m respectively.

Density, viscosity, and solubility of CO₂ are sensitive to temperature. A temperature of ca. 29 °C at 1200 m below sea floor has been reported from the Malm mines, located immediately north of the Beitstadfjord (Arne Myrvang, pers. comm. 2003).

4. RESERVOIR SIMULATION

4.1 Rationale

The goal of the reservoir simulation study is to find out if the Frohavet Basin may be suitable for safe and economically viable CO₂ storage. Given the lack of data on reservoir and seal properties, the approach chosen here is to carry out simulations applying a range of reservoir property parameters and to evaluate if a reasonable combination of these parameters yields a storage potential. If there exists a favourable parameter combination, it may be worth to make more detailed investigations, such as to drill an exploration well, determine the lithology in the basin, and to measure reservoir properties of rocks in the subsurface of the Frohavet. If there is no suitable parameter combination, the conclusion could be that this site is not suitable for underground CO₂ storage.

The conditions to be fulfilled for suitability of this site were:

- Only minor leakage of CO₂ during and after injection. Following Hepple & Benson (2002) a yearly leakage rate lower than 0.01 % of the total injected CO₂ may be acceptable. This would e.g. correspond to a cumulative leakage of 20% of the total injected CO₂ after 2000 years. However, leakage should ideally be especially low during the first few centuries when leakage would add to ongoing industrial emissions and leakage rates may increase somewhat later (Lindeberg 2003).
- Storage capacity for all or a large part of the emissions from a planned power station that is, up to a total of 50 million tonnes during 25 years of injection.

4.2 An outline of major expected processes in the reservoir

CO₂ injected into the subsurface will at normal pressure-temperature conditions have a density lower than water. Depending on the temperature and pressure gradients there will be a transition from gaseous (low density) to 'super-critical' (high density, but still lower than water) CO₂ at a certain depth. Due to the density difference between water and CO₂, there will be buoyancy-driven upward migration of CO₂ from the perforated or open part of the injection well until it reaches a barrier for migration. Such barriers are typically low permeable rocks for which high capillary entrance pressures have to be overcome to allow CO₂ migration into them. CO₂ will then accumulate below the barrier and spread laterally below it. If there are permeable pathways through the barrier, they will be exploited when reached and parts of the CO₂ will migrate upwards through them. If the barrier is inclined, the CO₂ will migrate below the barrier up-dip.

Some CO₂ will dissolve in formation water. This is however a slow process as compared to migration. The establishment of convection in the reservoir will improve dissolution (Lindeberg & Bergmo 2003).

If the formation into which CO₂ is injected is sealed completely, that is, if no formation water (and CO₂) can leave it (or at very low rates compared to the CO₂ injection rate), pore pressure in the reservoir formation will increase. If the pore pressure in the formation or in its seal rises locally above a critical pressure, hydraulic fracturing will occur (see below). Pore pressure rise will be strongly governed by the ratio between volume injected CO₂ and available pore volume in the formation; the lower this ratio is, the lower will the pressure increase be.

The process of gas entering a water-saturated, water-wet rock ('drainage') followed by subsequent re-entrance of water ('imbibition') is not symmetric but is strongly hysteretic. One consequence of this hysteresis is that a certain 'residual gas saturation' remains in the pore space. The residual gas is trapped and can leave the rock volume only by dissolution into the water phase and transport therein. This process reduces thus the amount of 'free' gas which might leak from the reservoir. In general, the higher the residual gas saturation (which is a function of the pore space geometry and of the previously reached maximum gas saturation) the larger the positive contribution to reservoir safety will be.

Hydraulic fracturing – maximum pore pressure condition

Hydraulic fracturing occurs when the minimum effective principal stress becomes smaller than the tensile strength of the material. The minimum effective principal stress is the minimum principal stress minus pore pressure. The condition to be fulfilled to avoid hydraulic fracturing is thus:

$$\sigma_3 - P_p \geq \sigma_T$$

where σ_3 is minimum principal stress (tensile is negative, compressive is positive), P_p is pore pressure, and σ_T is tensile strength.

In the Frohavet case, the maximum principal stress is probably the vertical stress (lithostatic stress, σ_v) and the minimum principal stress is accordingly the smallest horizontal stress (σ_h). A typical relationship between the vertical stress and the horizontal stress in such cases is

$$\sigma_h = c \cdot \sigma_v$$

where c is a constant and the vertical stress is

$$\sigma_v = \int_0^Z (\rho(z) \cdot g) dz$$

where Z is the depth for which vertical stress is calculated and ρ is the bulk rock density as a function of depth z .

The constant c is often taken to be of the order of 0.7 to 0.85 (e.g. Twiss & Moore 1992, Bjørlykke 1999). Here, an optimistic value of 0.85 was chosen.

4.3 Reservoir model and input data

Reservoir model

Based on the geological concept for the Frohavet Basin and the analysis of the available data on its sedimentary infill as presented in Chapter 3, a reservoir model has been generated (Figure 4.1) using the Irap RMS software package.

This model assumes two formations with suitable reservoir properties for CO₂ storage: seismic units B and C, for simplicity being termed 'Garn Formation' and 'Ile Formation',

respectively (Table 4.1). Seismic unit A ('Melke Formation') is assumed to be tight. All these formations are tilted with a general dip towards the SE.

The tilted formations are overlain by a thin Quaternary cover, which is partly absent and which is not considered to be a seal.

The seawater above the Quaternary cover was represented by a layer of cells with 100% porosity and very large volume, thereby simulating a large capacity for formation water or CO₂ migrating upwards from the basin.

The basement below the sedimentary succession is not included in the reservoir model. It is thus treated as impermeable.

Table 4.1 Seismic units, formations, and their status in simulations

Seismic unit	C	B	A	-	-
Formation/ Subgrid	'lle'	'Garn'	'Melke'	Quaternary	Water
Status in simulations	Active	Active	Inactive	Active	Active

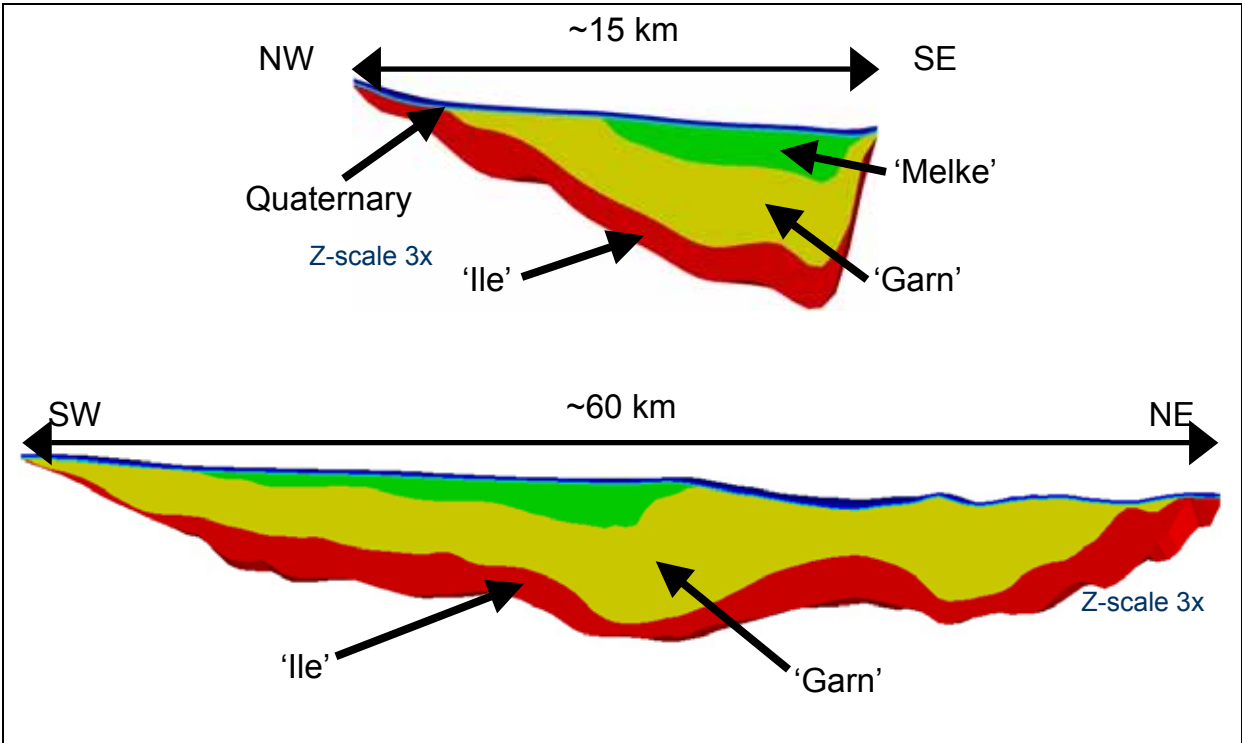


Figure 4.1 Cross-sections through the reservoir model of the Frohavet Basin (for location see Figure 4.2). The formation colour code is identical in the two cross-sections. The single-layer model representation of seawater is shown as a dark blue layer above the thin (light blue) Quaternary.

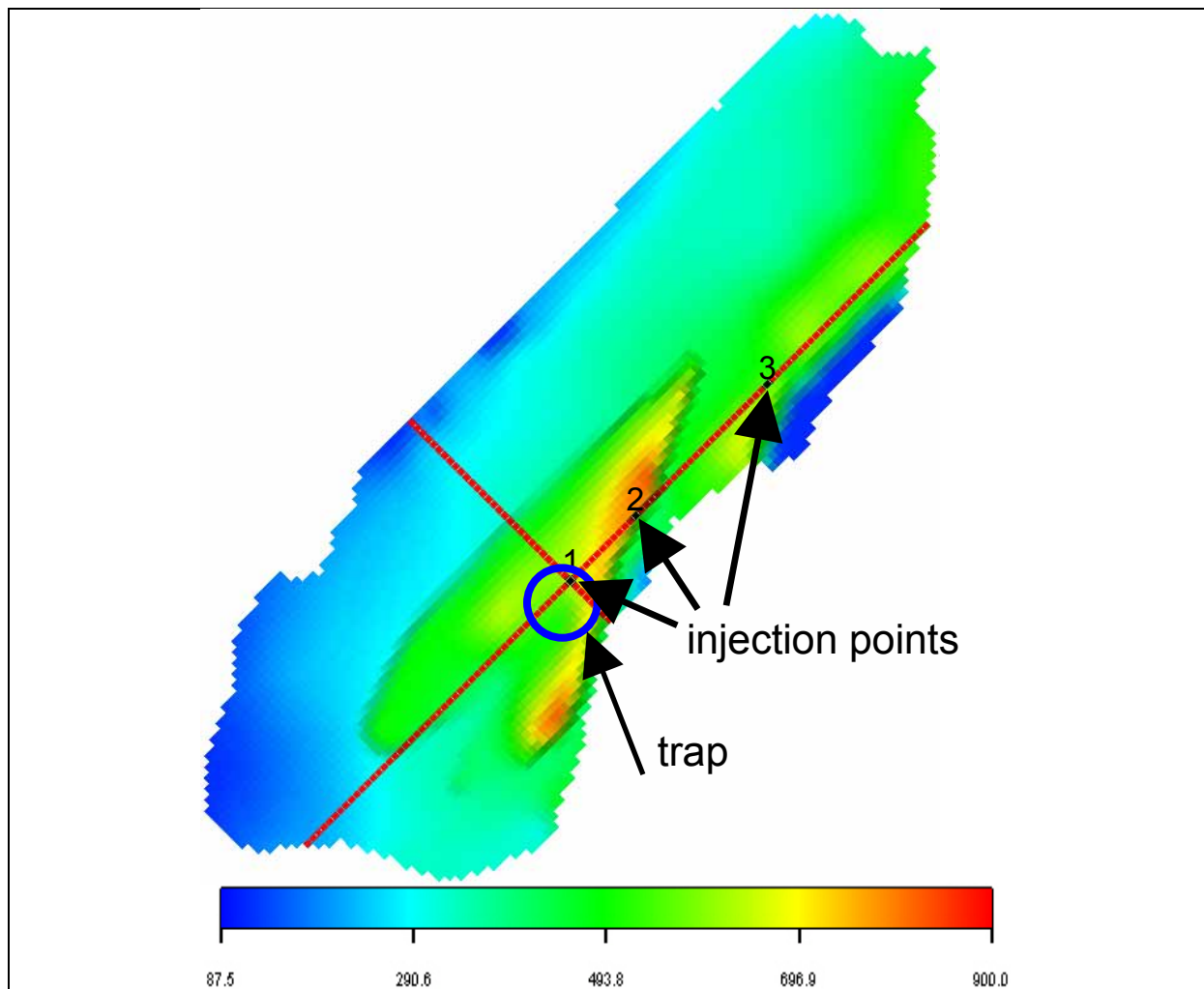


Figure 4.2 Depth to the top 'Garn' Formation. Red lines indicate cross sections (Figure 4.1) and arrows denote injection points used in simulations. Injection point 1 is the base case location.

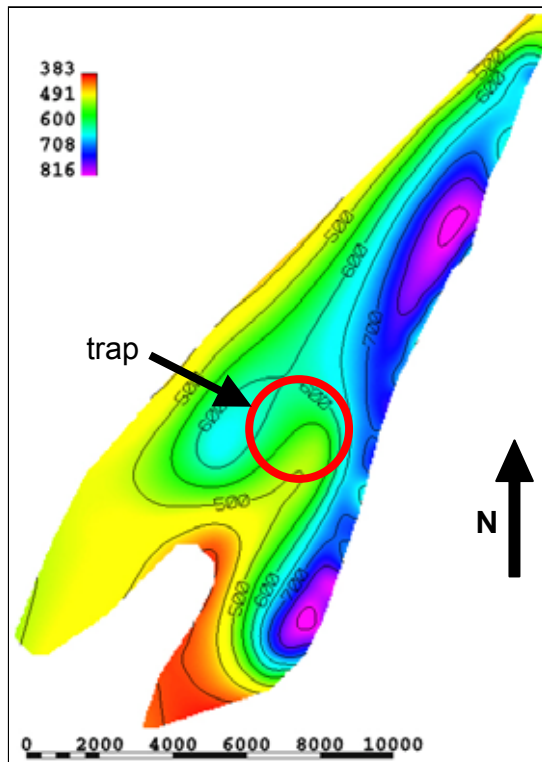


Figure 4.3 Depth map of the base of the 'Melke' Formation indicating a dipping anticline which serves as a trap in several simulations.

The primary input for reservoir geometry were four horizons from seismic interpretation (bathymetry = top Quaternary, top of seismic unit B = top 'Garn', top of seismic unit C = top 'Ile', and top basement = base of seismic unit C). One additional horizon (base of Quaternary) was added in order to represent a thin Quaternary layer which may have been below seismic data resolution. The Quaternary was represented by one layer with constant thickness of 15 m from the mapped sea floor downward.

The horizons define five formations or subgrids (Table 4.1): four sedimentary formations (Figure 4.1) and a water layer on the top. The subgrid with the tight 'Melke' Formation was treated as inactive. Lateral cell boundaries were always vertical. Cell dimensions were approximately 351 m in both NE-SW and NW-SE directions. The final model consists of 259 547 active cells. The reservoir properties (see below) are constant within each subgrid.

Table 4.2 Construction parameters for cells in the modelled formations in the subsurface geology model (Irap RMS).

'Formation'	Seismic unit	Internal geometry	Number of active cells
Water	–	1 layer, parallel to base	4629
Quaternary	Quaternary	1 layer, parallel to top	4629
'Melke'	A	None	inactive
'Garn'	B	10 m thick cells, parallel to base	126644
'Ile'	C	10 m thick cells, parallel to top	123645

Reservoir properties

Porosity and permeability of the formations in the Frohavet Basin are only poorly constrained due to the lack of samples. Based on the arguments given in Chapter 3, using analogy to the formations in hydrocarbon fields of the continental shelf offshore Mid-Norway, a range of parameters has been applied to the formations (Table 4.3). Base case values are similar to those reported in Ehrenberg (1990) and Koch & Heum (1995).

Table 4.3 Reservoir parameter range applied to the formations in the Frohavet Basin

Formation	Net-to-Gross ratio	Net porosity	Net horizontal permeability
Quaternary	1	20%	100 mD
'Melke Formation'	0 (inactive)	0 (inactive)	0 (inactive)
'Garn' Formation	0.75	25%, 12.5%	2000 mD, 20 mD
'Ile Formation'	0.75	25%, 12.5%	2000 mD, 20 mD

Vertical heterogeneity within the formations was represented by a ratio of 0.1 (1 / 10) between vertical and horizontal permeability (k_v and k_h respectively). In addition the effect of applying a k_v/k_h ratio of 0.01 was tested.

No dependency of saturation to capillary pressure was assumed for most of the simulated cases. Accordingly the entry pressure of CO₂ into reservoir and seal rocks is 0 and saturation is not affected by the capillary pressure. However in some simulations a dependency of gas and water saturation in the reservoir formations on capillary pressure was applied in order to check its influence on results.

Reservoir conditions

A seawater temperature of 8° C was assumed. This corresponds accordingly to the temperature at the sea floor, which is in the Frohavet on average at approximately 320 m bsl. Temperature measurements at the Malm mines a few km north of the Beitstadfjord yielded

29° C at 1200 m bsl. (A. Myrvang, pers. comm. 2003). The calculated temperature gradient for the Frohavet is accordingly 23.9° C/km (Figure 4.4). Note, that the temperature gradient may in reality be higher at the Frohavet, because it is situated closer to the continental margin (with usually higher temperature gradients) than Beitstadfjorden.

Pore pressure at injection start was assumed to be hydrostatic (Figure 4.4).

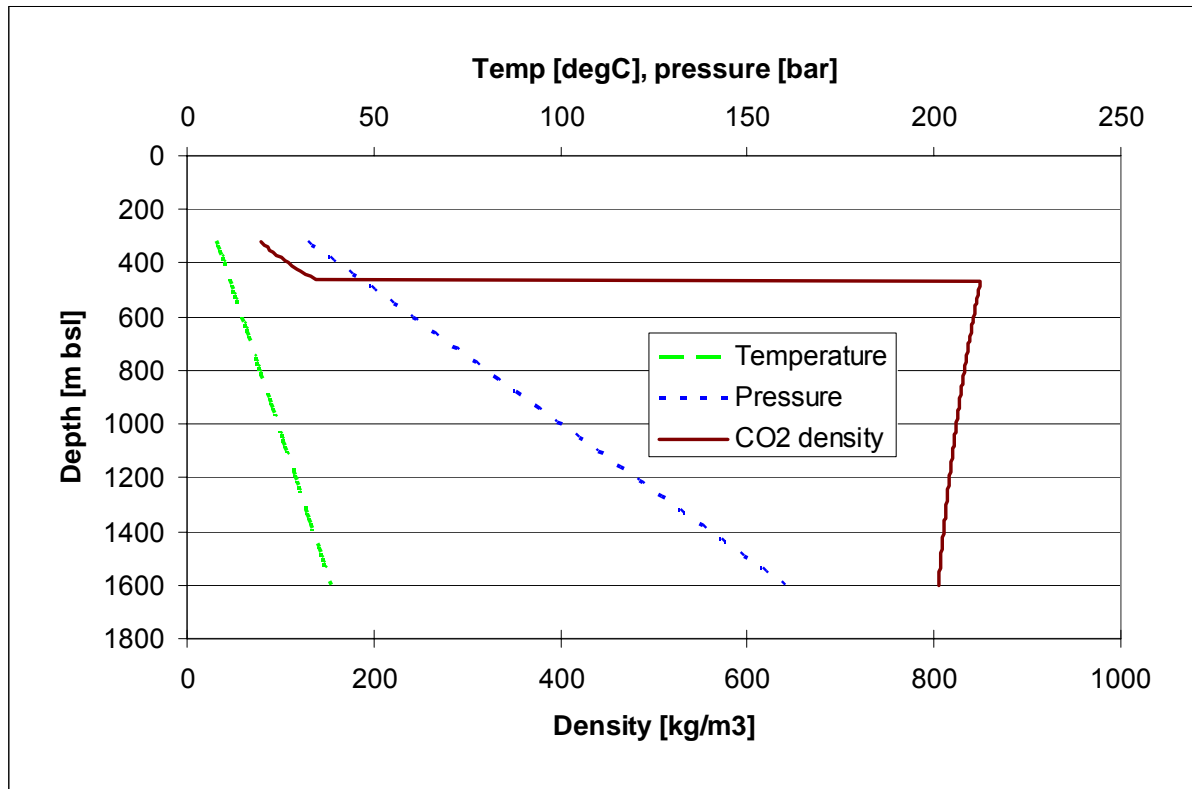


Figure 4.4 Calculated temperature, pore pressure and pT -dependent CO_2 density versus depth for the Frohavet Basin.

Fluid properties

Density and viscosity of water and CO_2 were calculated using SINTEF's thermodynamic model for the CO_2 - CH_4 - H_2O system (Lindeberg et al. 2000). For simplicity and to be able to handle isothermal pressure variations in the reservoir (due to injected CO_2), an isothermal model was used with a fixed temperature of 29° C (Figure 4.5) which corresponds to the depth of 1200 m bsl for the temperature gradient used. The (non-isothermal) density variation with depth for the calculated temperature and pressure profiles is shown for comparison in Figure 4.4. The major feature of interest is the strong downward density increase at approximately 450 m bsl, below which CO_2 density is higher than 800 kg/m^3 .

Figures illustrating the variation of water density with pressure and the dependency of viscosity on pressure and temperature are provided in Figure 4.6, Figure 4.7, and Figure 4.8.

Dissolution of CO_2 into water is according to the model of Enick & Klara (1990).

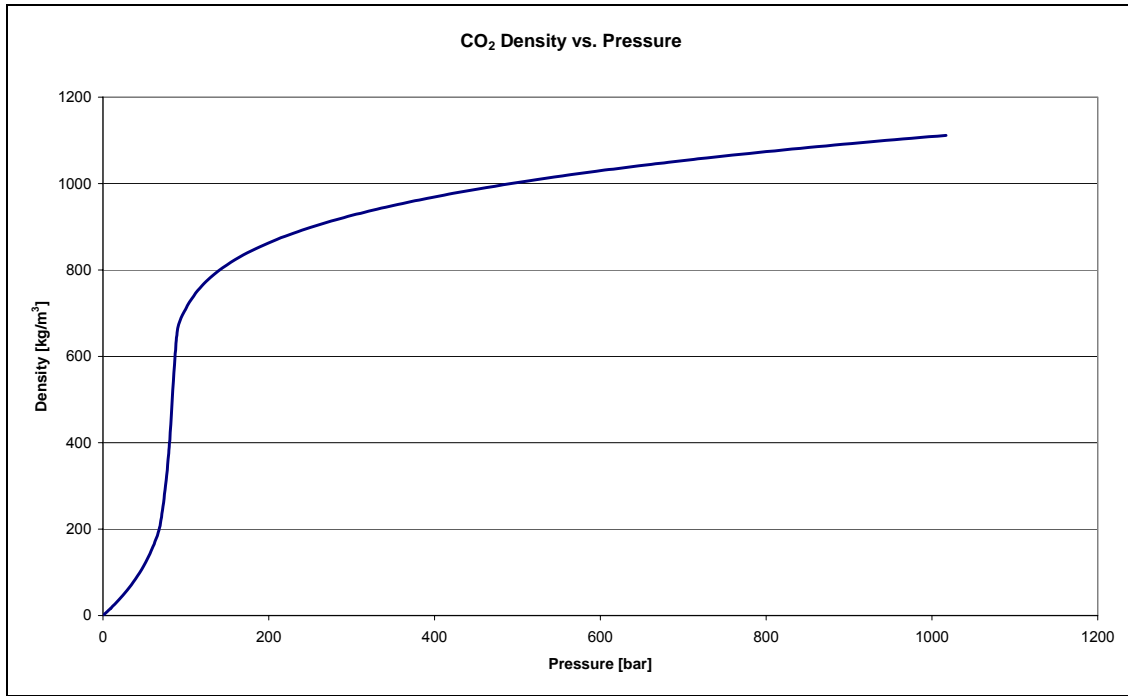


Figure 4.5 *CO₂ density vs. pressure at reservoir temperature of 29°C.*

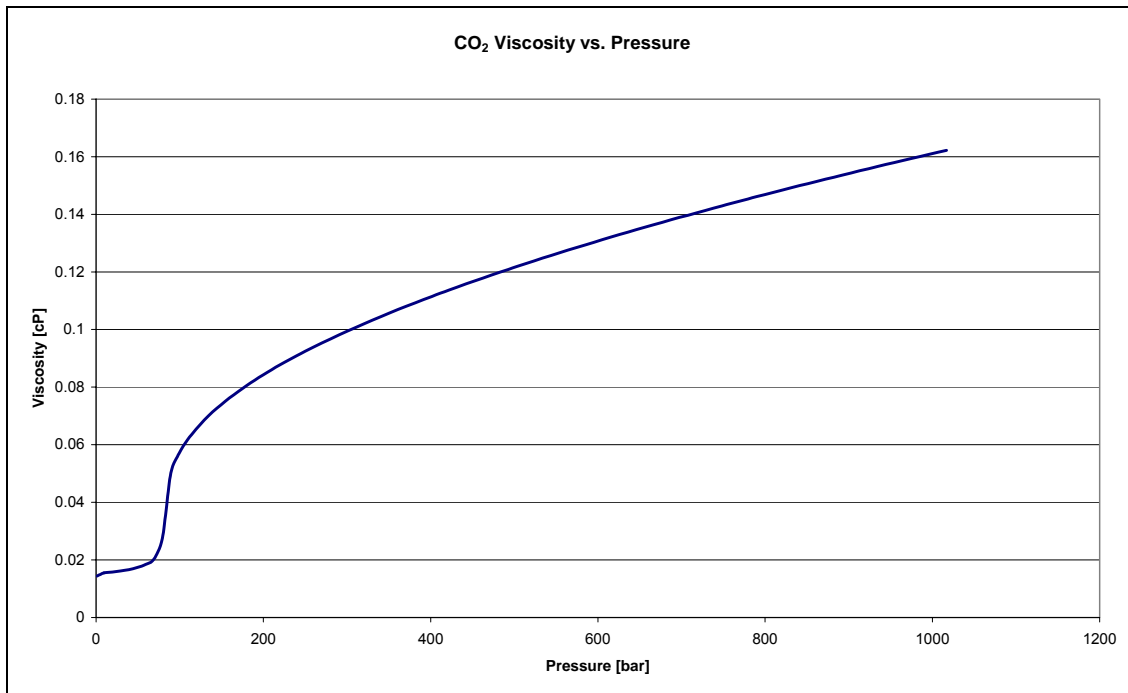


Figure 4.6 *CO₂ viscosity vs. pressure at reservoir temperature of 29°C*

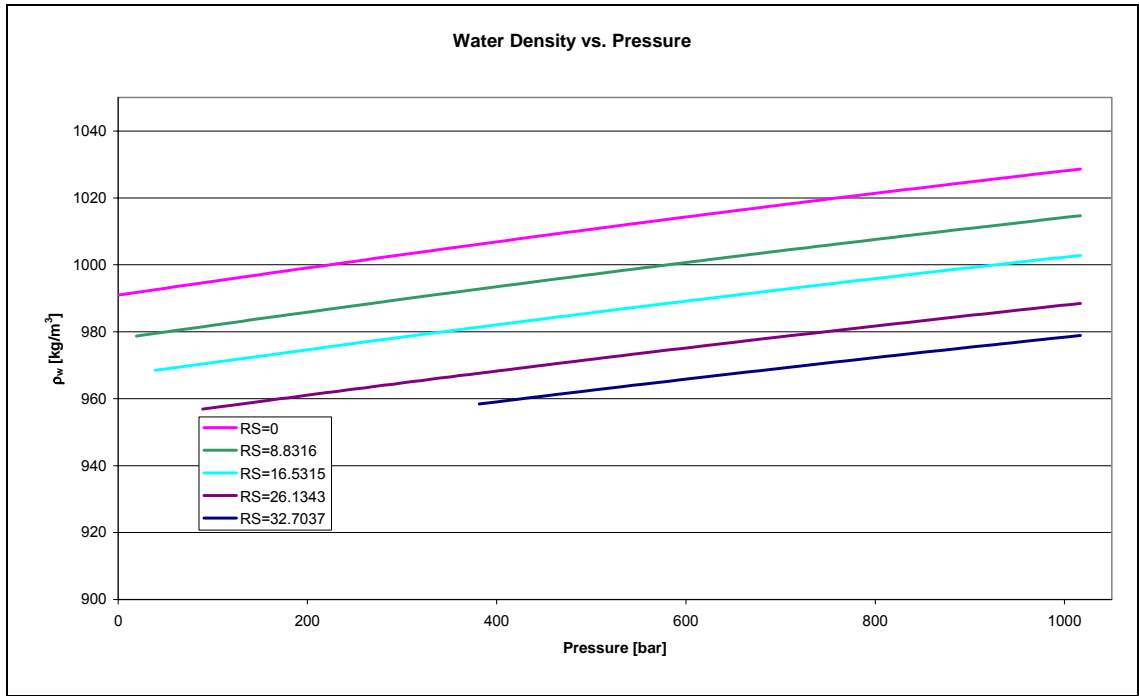


Figure 4.7 Density of reservoir water at different CO_2 saturation vs. pressure at reservoir temperature of $29^\circ C$

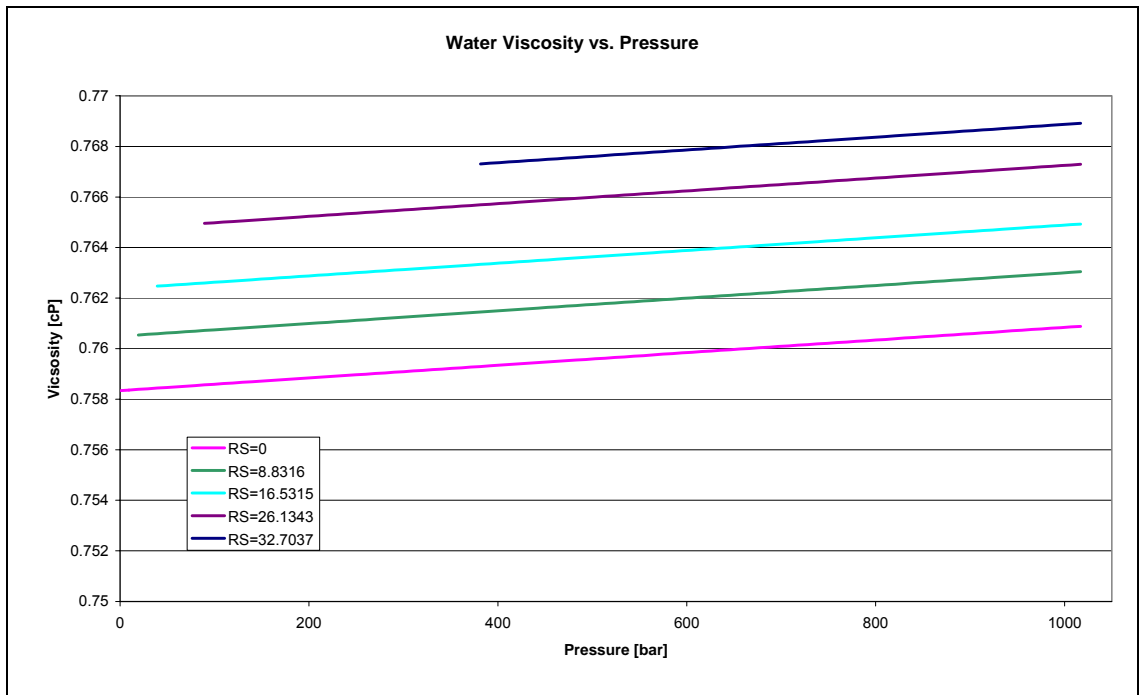


Figure 4.8 Viscosity of reservoir water at different CO_2 saturation vs. pressure at reservoir temperature of $29^\circ C$

Relative permeability and capillary pressure curve

Base case relative permeability curves used for water and CO₂ in the water-CO₂ system are shown in Figure 4.9. They are taken from core experiments with samples from the Utsira Formation in the Sleipner field (partly documented in Lindeberg et al. 2000). The base case CO₂ relative permeability curve corresponds to an irreducible water saturation of 0.1 and a residual CO₂ saturation in imbibition of 0. In some simulations different sets of relative permeability curves were tested (see below). All relative permeability curves assume no hysteresis effects (identical curves for drainage and imbibition).

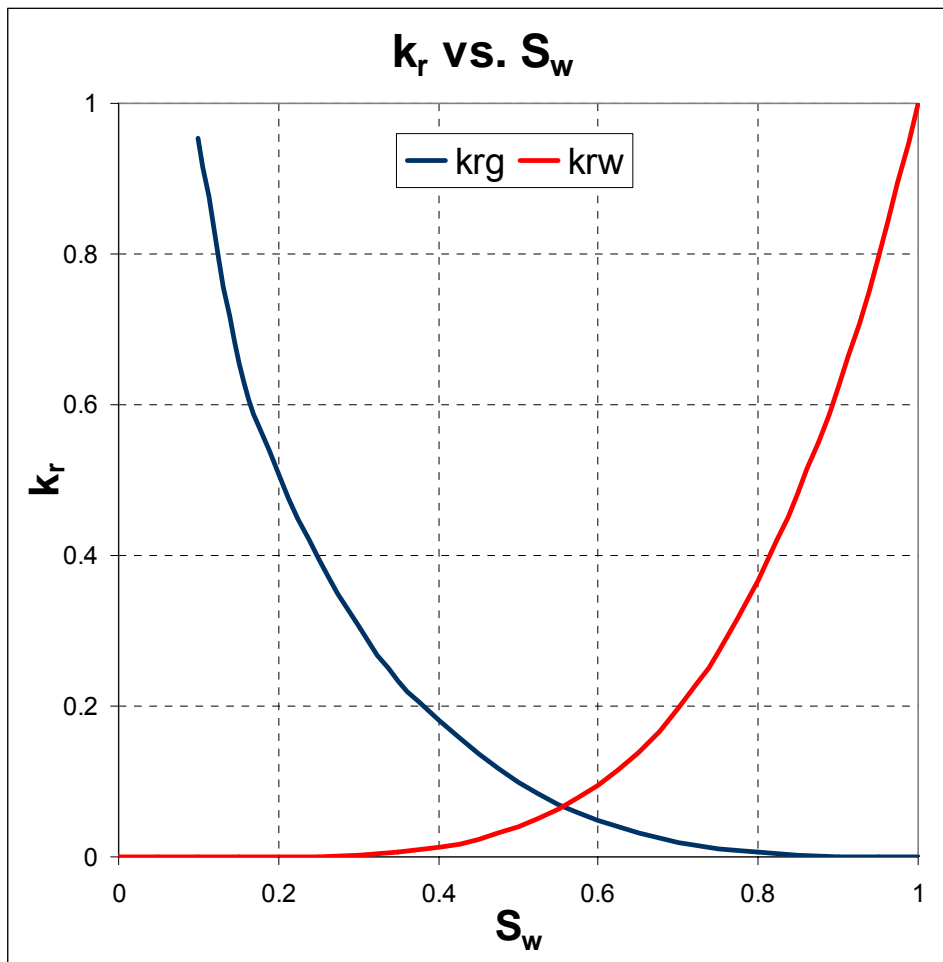


Figure 4.9 Relative permeability curves used for water and CO₂ in the water-CO₂ system

Calculated reservoir volume

The constructed reservoir model has for the base case (Net-to-Gross ratio of 0.75 and net porosity of 25 %) the volumes listed in Table 4.4.

Table 4.4 Calculated reservoir volumes (in Eclipse) in 10^6 m^3

Formation	'Ile'	'Garn'
Bulk volume	135647	139794
Total pore volume	25434	26211

Other simulation specifications

Reservoir simulation was carried out with the commercial 'Eclipse 100' black-oil simulator.

The wells were treated as vertical. The well positions and perforations for injection are placed at positions that are expected to result in the slowest migration or the longest migration path to the surface. Such positions are below an inclined anticlinal trap and at the deepest part of the basin, in both cases with perforations immediately above the top of the basement.

The injection rate was defined as 2 million tonnes/year which corresponds to $2.93 \cdot 10^6 \text{ Sm}^3/\text{day}$ and a total of $26.7 \cdot 10^9 \text{ Sm}^3$ over a period of 25 years.

The diffusion option of the Eclipse software was not applied because the effect of diffusion is negligible in short term simulations.

Most simulations were run for 50 years, which is until 25 years after the end of simulated injection. There were also runs for 2000 and in one case 10 000 years in order to investigate the long-term CO_2 behaviour in the most promising cases, that is when there was no or small leakage during the first 50 years.

4.4 Simulation results – predicted leakage rates

The simulations are grouped into two sets:

- Base case which serves as a kind of ‘worst case’ scenario.
- Alternative cases in which reservoir properties were changed in order to test their potentially beneficial effect to reduce leakage of CO₂.

4.4.1 Base case

Reservoir properties in the base case run correspond to those used in the Beitstadfjorden study (Polak et al. 2004) since the same geological formations are considered. Parameters used in the base case simulation are shown in Table 4.5.

Table 4.5 Parameters used for simulation in the base case.

Parameter	Value
Injection rate [Sm ³ /day]	2 930 188.26
Injection time [years]	25
Net porosity in reservoir	0.25
k _h in reservoir [mD]	2 000
k _v in reservoir [mD]	200
NTG in reservoir	0.75
S _w (P _c)	no dependency

k_h = horizontal permeability, k_v = vertical permeability,
NTG = net-to-gross ratio,
S_w(P_c) = water saturation as function of capillary pressure

The injection point for the base case was carefully chosen according to the geological structure of the basin and is placed at the base of the ‘Ile’ Formation vertically beneath a mapped dipping anticlinal trap (Figure 4.1, Figure 4.2 and Figure 4.3). However, the pore volume in the trap is small such that only a small fraction of the injected CO₂ can be stored in it. Accordingly, the simulation predicts a very high cumulative volume of CO₂ to migrate from the trap towards the sea floor and to leak from the reservoir. Leakage is predicted to start already after 10 years of injection and around 86% of the total injected CO₂ would have escaped during 50 years after injection started (Figure 4.10). The main reason for such a rapid leakage is the high permeability of the reservoir formations. Given the base case reservoir parameters, the Frohavet Basin would not be suitable for long-term CO₂ storage.

Figure 4.11 illustrates the general behaviour of most of the simulated cases: CO₂ is injected into the ‘Ile’ Formation and reaches a saturation plateau there. It soon migrates into the overlying ‘Garn’ Formation, from where it starts to leak into the sea. Decreasing stored amounts in the reservoir formations after 25 years are due to ongoing leakage while injection has ended.

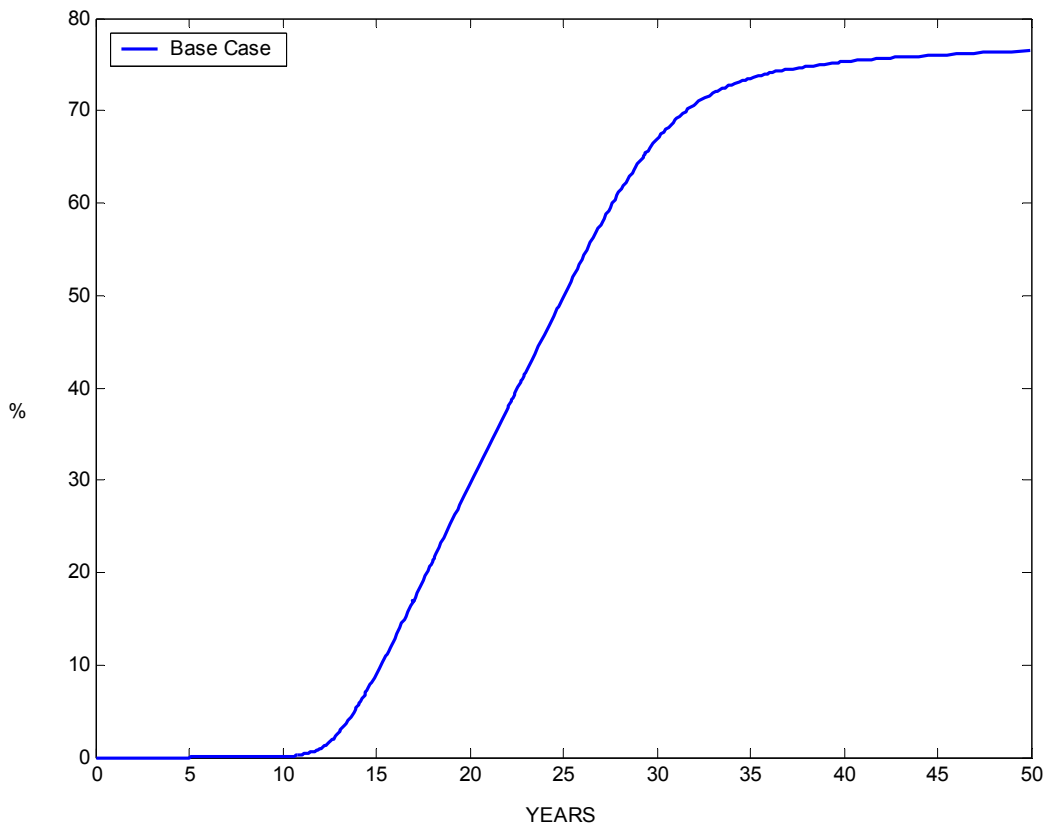
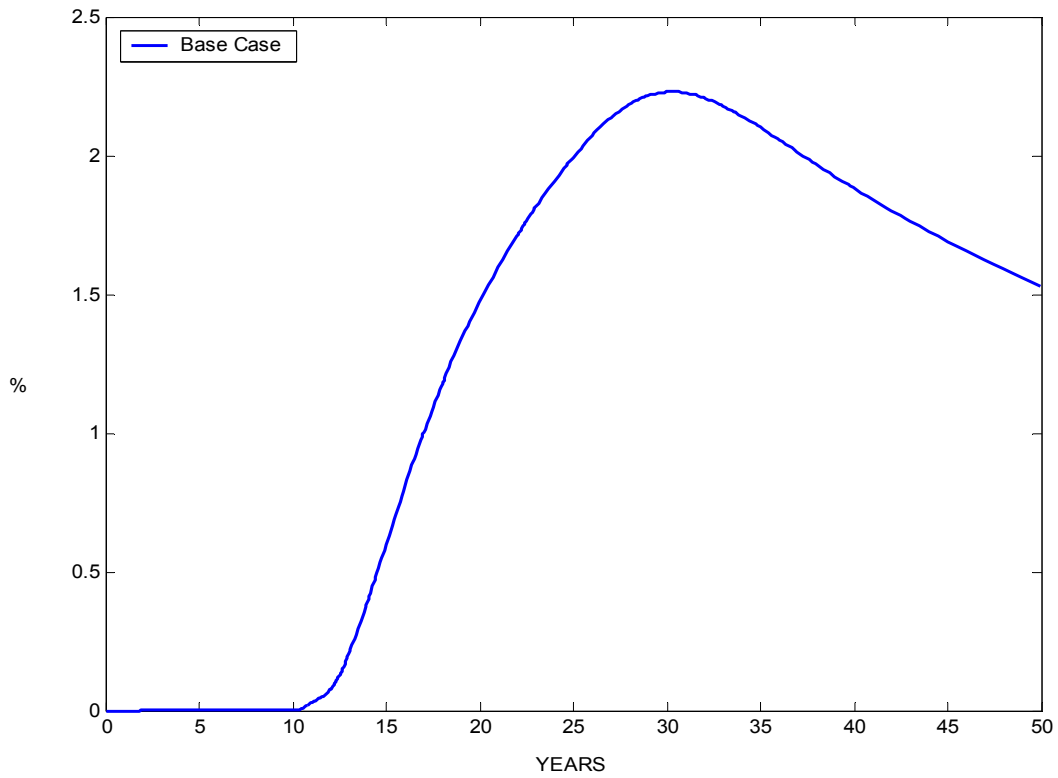


Figure 4.10 Simulated fraction of total injected CO₂ (%) predicted to have leaked from the reservoir for the base case; as fraction of the total injected amount). Upper: annual rate, lower: cumulative leakage.

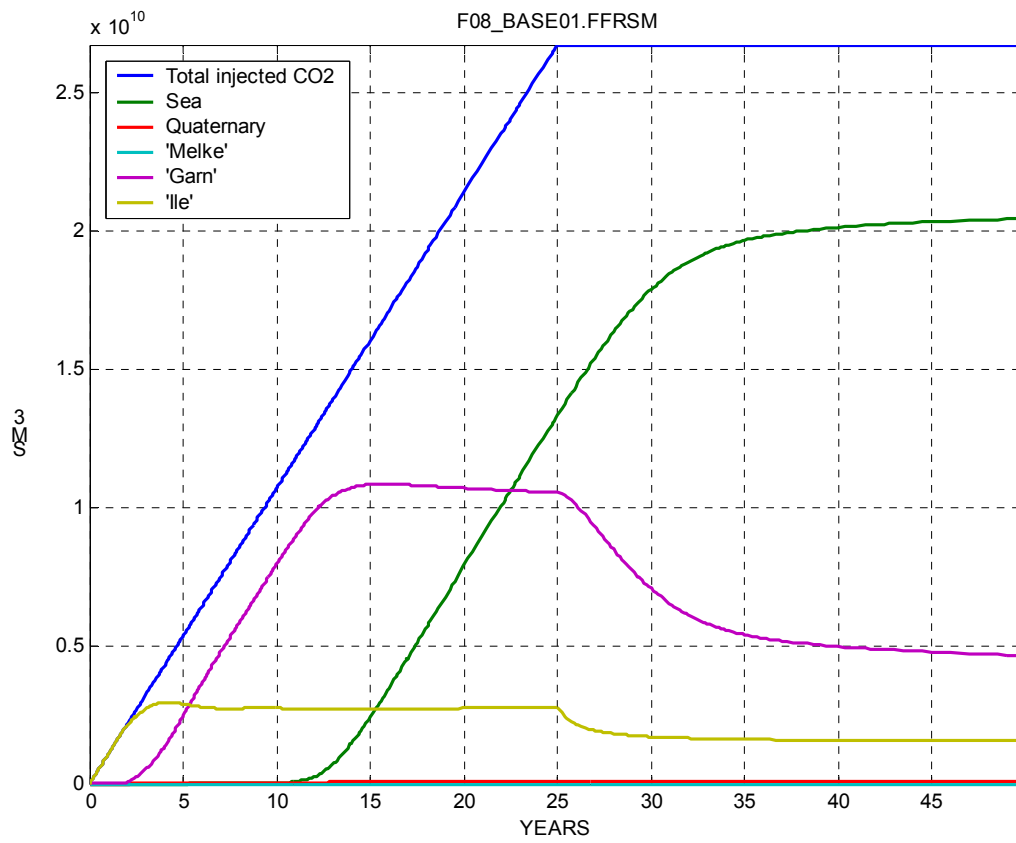


Figure 4.11 Simulated quantities being injected and stored in the various formations in the model. The amount stored in 'Sea' is the leaked part. y-axis: volume in 10^{10} m^3 .

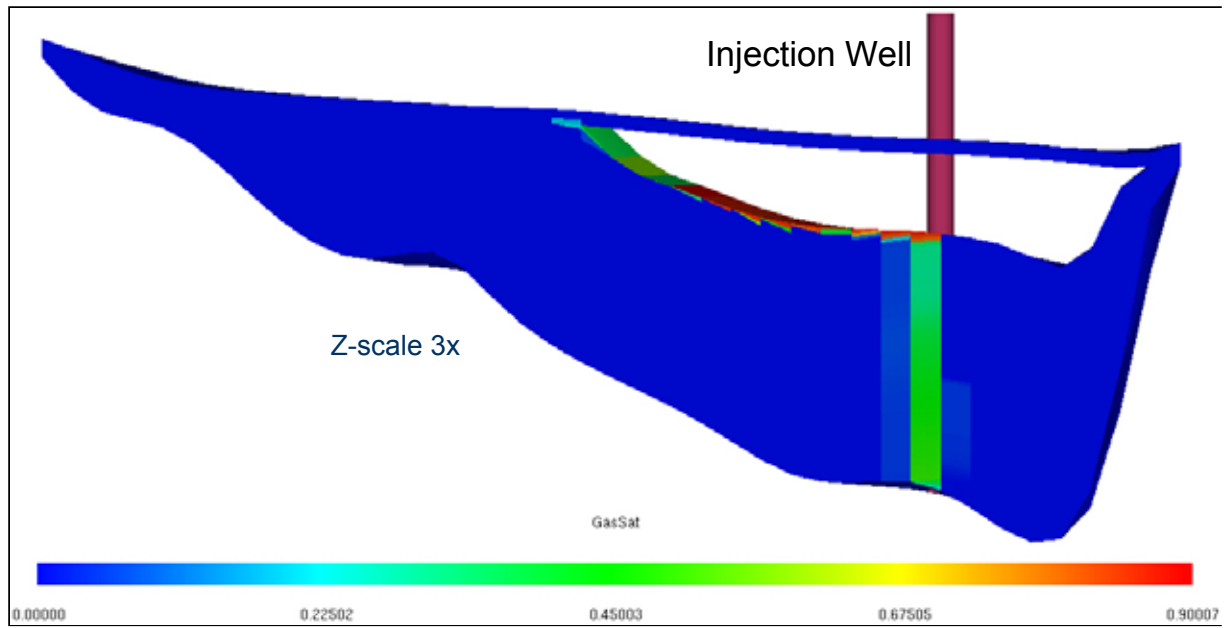


Figure 4.12 Gas saturation in the reservoir after 25 years of CO₂ injection. NW is left.

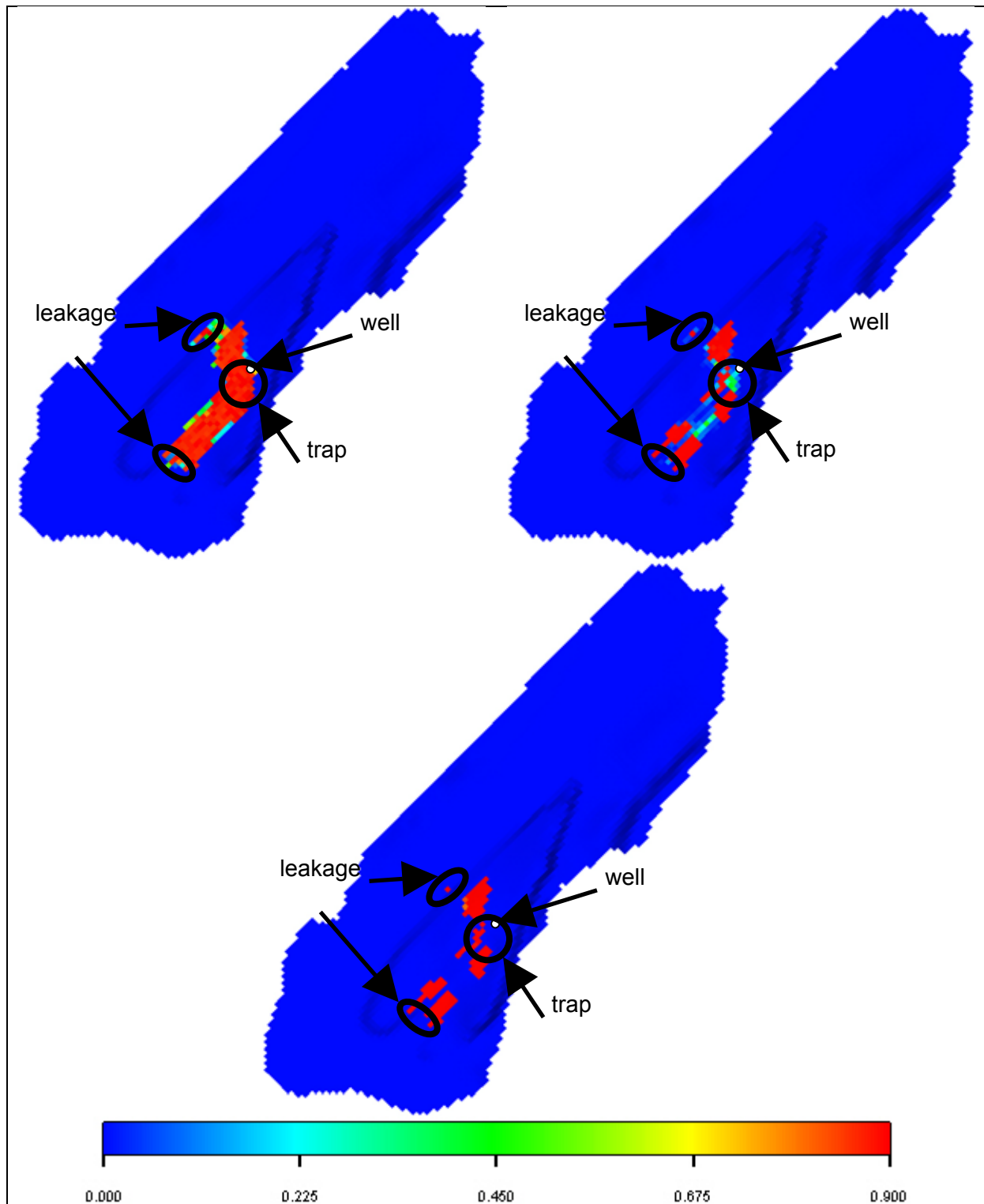


Figure 4.13 Gas saturation at the top of the 'Garn' Formation after 25 years (upper left), 100 years (upper right) and 2000 years (lower).

4.4.2 Alternative cases

The base case constitutes a ‘worst case’ scenario for CO₂ storage in the Frohavet Basin. Alternative cases were simulated with the aim to investigate if reasonable combinations of reservoir parameters may exist at which this site could be suitable for CO₂ storage. The following modifications to the base case have thus been applied:

- reduced reservoir permeability and associated porosity
- reduced k_v/k_h ratio in the reservoir
- different location of the injection point
- two injection wells instead of a single one
- different sets of relative permeability curves including changes in residual gas saturation (S_{gr}) and a dependency of water and gas saturation on capillary pressure
- lower absolute permeability in the upper part of the reservoir (‘Garn’ Formation)
- reduced injection rate.

Reduced permeability and porosity

A reduction in absolute permeability will reduce migration velocity and will thus likely reduce leakage rates. However, porosity and permeability are linked to each other, with a general trend in reservoir rocks of lower permeability corresponding to lower porosity. Lower porosity implies less pore space available for CO₂ and thus potentially an increased migration rate. Porosity and permeability were here changed in a way to maintain a reasonable relationship between these two parameters.

When porosity is reduced to the half and permeability reduced 100 times as compared to the ‘base case’, leakage is predicted to start much later, around 200 years after beginning of injection (curve #2 in Figure 4.14). However, the long term simulation indicates that after 2000 years 45% of the total injected gas would have escaped from the reservoir. Thus, considerably reduced porosity and permeability yield more favourable results than the base case but they are still far from fulfilling conditions that would be required to accept this site as suitable for long-term storage of CO₂.

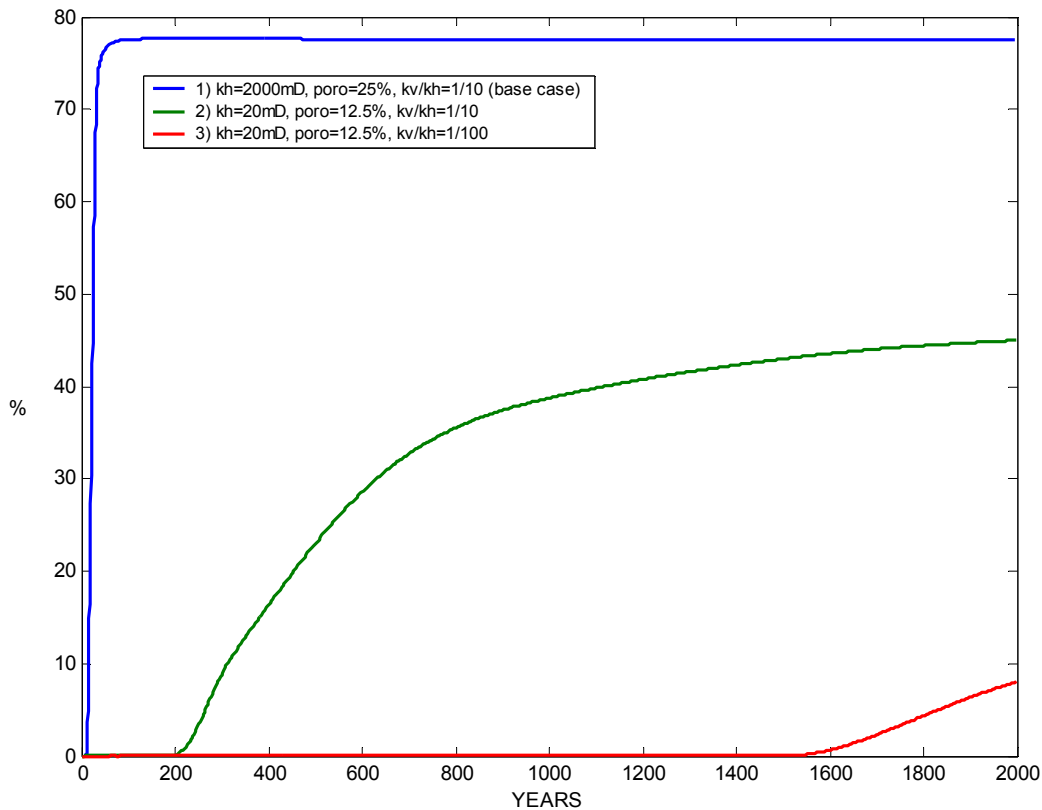


Figure 4.14 Simulated fraction of total injected CO₂ predicted to have leaked from the reservoir; effect of changes to the absolute permeability, porosity and k_v/k_h ratio

A lower ratio between vertical and horizontal permeability (k_v/k_h) is expected to result in slower upward migration of CO₂ across the sedimentary layers. The simulation shows that the effect on the prediction is significant (Figure 4.14). Leakage of CO₂ is predicted to start about 1350 years later in this case than in the previous one, that is after about 1550 years. Also the predicted volume of leaked gas is much lower and after 2000 years only about 7% of the total injected CO₂ is predicted to have escaped. However the steep slope in the curve of the cumulative leakage for the last simulation in Figure 4.14 suggests that the volume of leaked gas will continuously increase in the following centuries or even millennia, though with gradually decreasing annual leakage rates. The predicted cumulative leaked fraction after 2000 years corresponds to an overall average leakage rate of 0.0035 % per year and is thus below the limit suggested by Hepple & Benson (2002). The average annual leakage fraction during the 450 years leaking period from 1550 to 2000 years after injection start is 0.016 %.

The results from this group of simulations show that absolute permeability and the k_v/k_h ratio are important parameters influencing the leakage rate profile. Given a moderate to low permeability and a low k_v/k_h ratio it may be possible to keep CO₂ in the reservoir for sufficiently long time before it will start to escape.

So far, very little is known about the sedimentary rocks in the Frohavet Basin and their reservoir parameters. Neither absolute permeability of individual layers, nor the type of vertical or horizontal heterogeneity is known and thus no confident estimate of k_v/k_h can be

made. An appraisal of the validity of the simulations would therefore require acquisition of well data and cores and analyses of core samples.

Well location/injection point

The time to the start of leakage can be increased significantly if the injection point is carefully chosen. The seismic horizon for the top of the 'Garn' Formation indicates the presence of a dipping anticlinal trap (Figure 4.2 and Figure 4.3). Most simulations were carried out with an injection point located below that trap. In order to see the effect of a different well location a simulation was made with the injection point located in the deepest part of the reservoir (location #2 in Figure 4.2). This simulation is a variation of the case with moderate to low permeability (20 mD, 12.5% porosity) but with high k_v/k_r ratio (0.1, middle curve in Figure 4.14).

Figure 4.15 shows that the trap is predicted to help to delay leakage but finally less gas would escape in the case in which the well is located at the deepest part of reservoir. This result in the latter case is caused mostly by dissolution of CO₂ in water. In this latter case, the pore space volume that is reached and partly saturated by CO₂ is larger and the CO₂ has a longer migration distance to the sea floor than in the case of injection below the trap. A larger size of the 'bubble' means a larger contact surface between gas and water which results in an increase of CO₂ dissolution in water. Although the different choice of the injection location improved the results, the average annual leakage rate of 0.02% (40% cumulative over 2000 years) and much higher annual leakage rates in the first centuries indicate that this scenario still does not fulfil the requirements for a safe long-term CO₂ storage site.

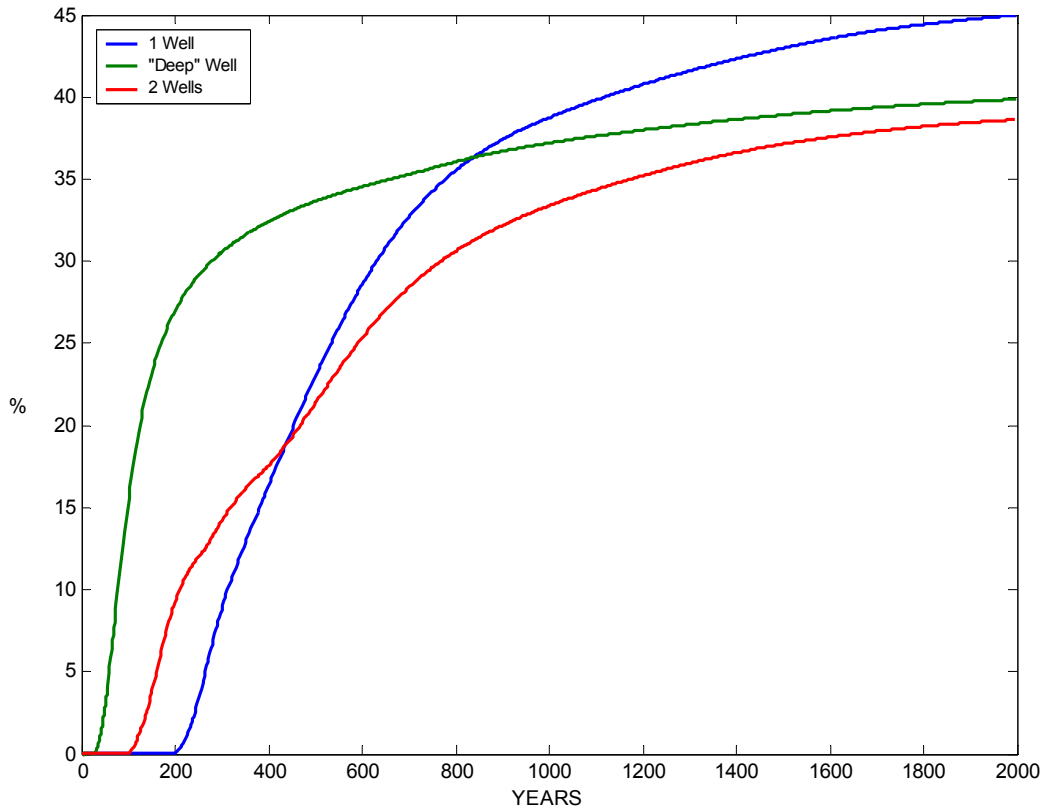


Figure 4.15 Simulated fraction of total injected CO₂ predicted to have leaked from the reservoir; effect of different location of injection points and effect of number of injection wells. All curves: $k_h = 20$ mD, $poro = 12.5\%$, $k_v/k_h = 0.1$.

Number of wells

Similarly in principle to the effect achieved in the previous simulation, distribution of the injection to two wells may enlarge the volume ‘touched’ by CO₂ and may thus enhance dissolution and reduce leakage. A simulation was thus carried out with two injection wells in different basin areas (locations #1 & #3 in Figure 4.2). The simulation results show that leakage would start in the two-well case at approximately 100 years (Figure 4.15), which is later than in the case with the single well positioned deepest in the basin but earlier than in the case with the single well below the dipping anticlinal trap. The cumulative leakage rate is predicted to be about 38% that is slightly lower than in the case of a single well positioned deepest in the basin.

The two-well case does not fulfil the criterion of Hepple & Benson (2002); it has an average annual leakage rate of 0.019% (38% over 2000 years) and much higher annual leakage rates in the first centuries. However, the more gentle profile of the leakage rate over time shows that this case is more favourable than the single-well case (well in the deepest part of basin). In general, this result indicates that a careful choice of injection locations may contribute significantly to the performance of the site.

Alternative relative permeability curves and application of a S_w - P_c relationship

The shape of relative permeability curves determines the migration velocity, the maximum gas saturation achievable, and the residual gas saturation. The effect of these changes has been tested by applying two alternative sets of relative permeability curves (Figure 4.16). The curves were assumed to be the same for drainage as for imbibition. Corey's equations for calculating gas and water relative permeability curves were employed (Corey 1976). The equation for water relative permeability (k_{rw}) is:

$$k_{rw} = (S^*)^\varepsilon \text{ for } 0 \leq S^* \leq 1 \text{ where } S^* = \frac{S_w - S_{wr}}{1 - S_{wr}}$$

S_w is the water saturation, S_{wr} is the irreducible water saturation and ε is a parameter.

For the gas relative permeability curve (k_{rg}) the equation is:

$$k_{rg} = (1 - S_h)^2 (1 - (S_h)^\gamma) \text{ for } 0 \leq S_h \leq 1 \text{ where } S_h = \left(\frac{S_w - S_{wr}}{1 - S_{wr} - S_{gr}} \right)$$

S_{gr} is the residual gas saturation and γ is a parameter.

The capillary pressure curve is based on van Genuchten's equation (van Genuchten 1980):

$$P_c = P_0 \left((S^*)^{-1/\lambda} - 1 \right)^{1-\lambda}$$

P_0 is a parameter and S^* is the same as in Corey's equation for water relative permeability.

All parameters used for each of the two new sets of curves are given in Table 4.6. They follow the values of 'Case 1' of Ennis-King et al (2002) to enable comparison. For the residual gas saturation, two cases are simulated with the aim to test the influence of this parameter on results.

Other parameters used in these simulations are as in the base case: reservoir permeability of 2000 mD, reservoir porosity of 25% and k_v/k_h ratio of 0.1.

Table 4.6 Parameters used in calculation of alternative relative permeability curves and a capillary pressure curve.

Case	S_{wr}	S_{gr}	ε	γ	P_0	λ
1	0.11	0.05	3.070	0.686	2.03	0.234
2	0.11	0.10	3.070	0.686	2.03	0.234

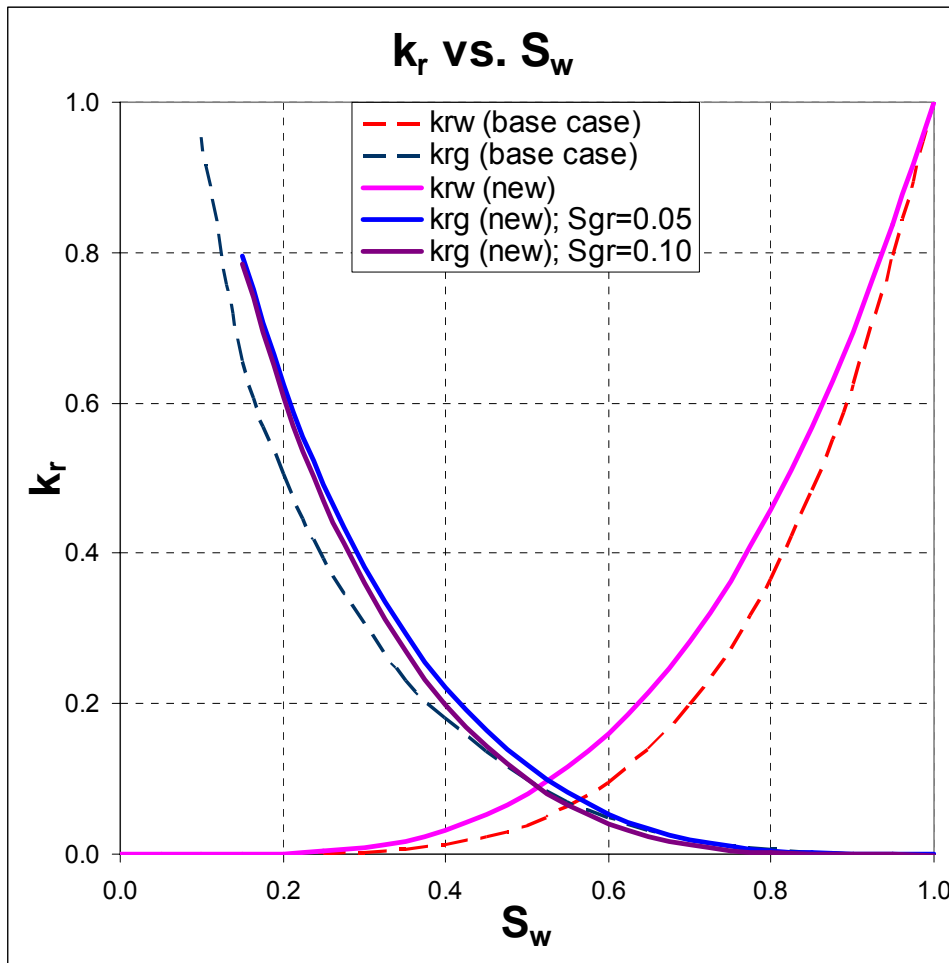


Figure 4.16 Base case and alternative relative permeability curves used for water and CO₂ in the water-CO₂ system. For parameters see Table 4.6.

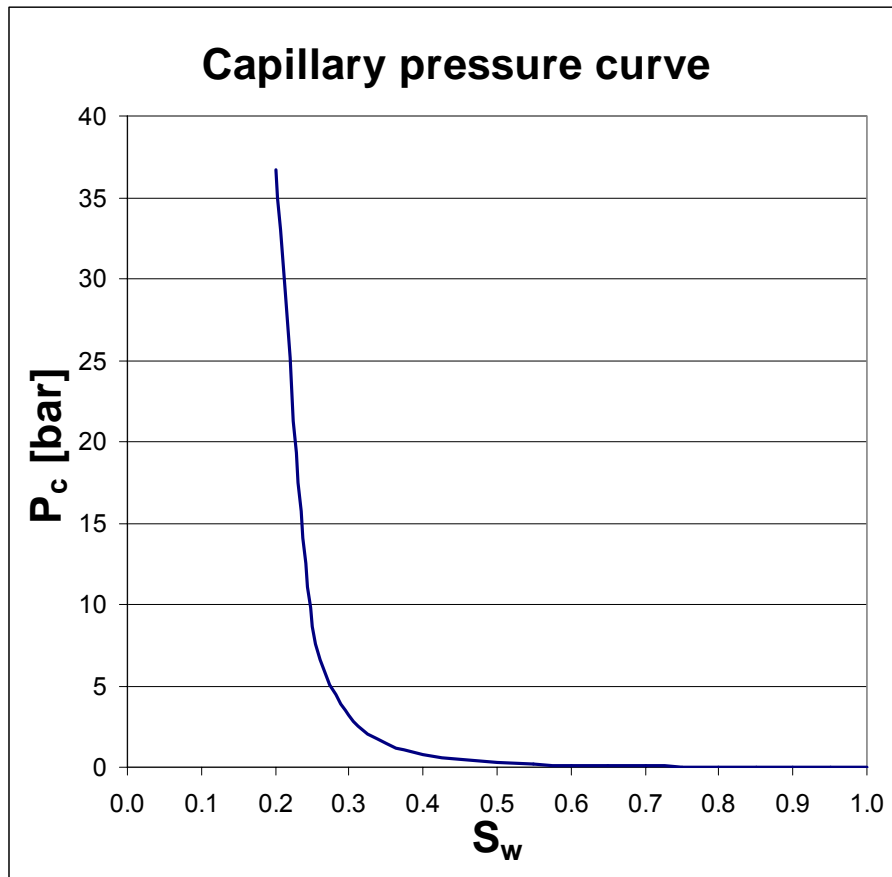


Figure 4.17 Capillary pressure curve for irreducible water saturation of $S_{wr}=0.11$. For parameters see Table 4.6.

Application of the alternative sets of relative permeability curves causes rather a change to the worse in the predicted results when no dependency of gas and water saturation on capillary pressure is employed (Figure 4.18). The predicted cumulative leaked fractions for the two alternative curves are only slightly different from that in the 'base case'. However, leakage is predicted to start earlier and to have higher leakage rates during the early years in the alternative cases than in the base case. This is caused by improved mobility of both water and gas (larger k_r values at the same S_w value for most parts of the alternative curves than for the base case curves, Figure 4.16). The predicted cumulative leakage for the case with the alternative relative permeability curve with $S_{gr} = 0.1$ is slightly lower during the final years than that for the base case. This is probably due to the slightly lower relative gas permeability in the alternative case for low gas saturations (high water saturations, $S_w > 0.5$, Figure 4.16), which seems to retard gas flow in the long term.

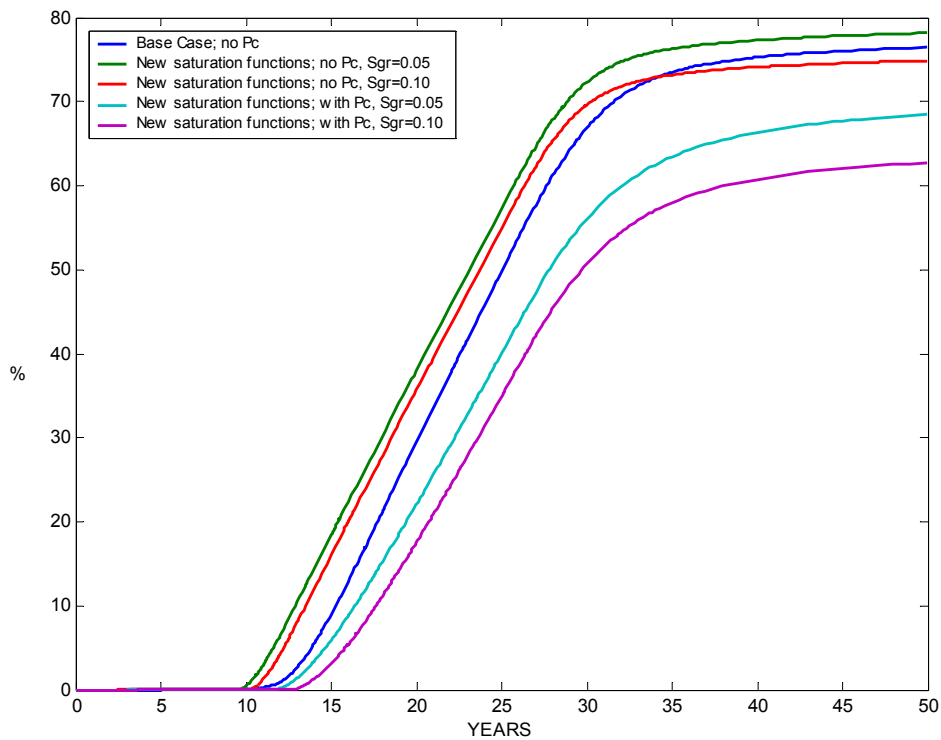
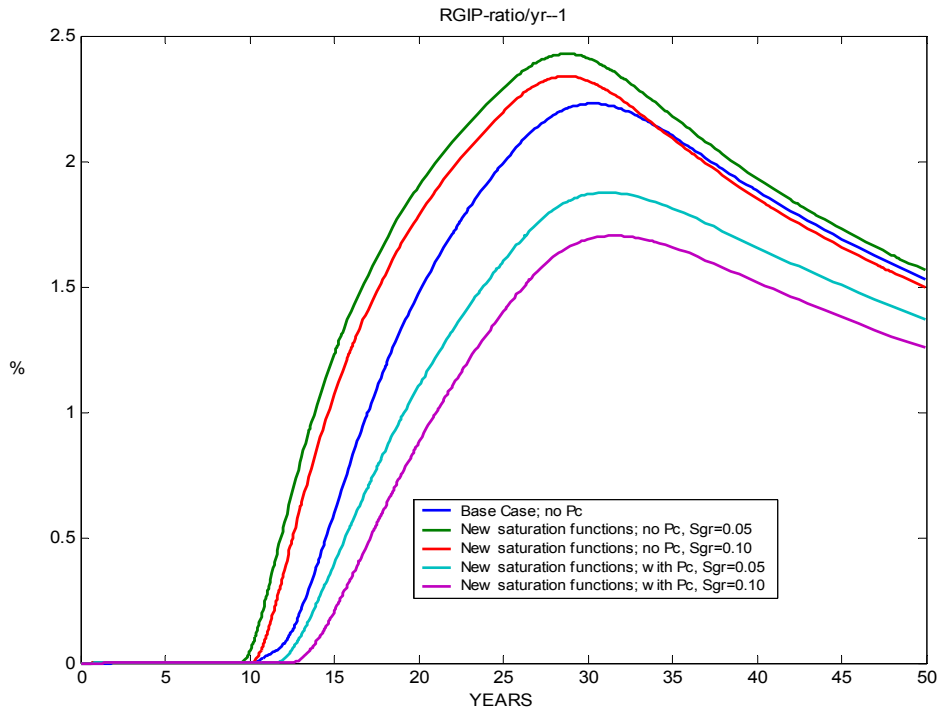


Figure 4.18 Simulated fraction of total injected CO₂ (%) predicted to have leaked from the reservoir; effect of use of alternative relative permeability curves and of dependency of gas and water saturation on capillary pressure ('with Pc', versus 'no Pc'), leaked amount shown as fraction of the total injected amount. Upper: annual rate, lower: cumulative leakage.

When a dependency of gas and water saturation on capillary pressure (Figure 4.17) is applied, the simulation results exhibit significant improvements (Figure 4.18). The onset of leakage is slightly delayed, annual leakage rates are lower, and the cumulative leaked fraction after 50 years is lower by about 10-12% as compared to the simulations without capillary pressure dependency. This difference is caused by a reduced migration velocity which is a consequence of the need to establish high capillary pressures to achieve high gas saturations (at which gas relative permeability becomes high). The case with the higher value of S_{gr} (residual gas saturation) exhibits a lower leakage rate and lower cumulative leakage fraction because more CO₂ is left behind trapped in the pore space.

Variations in relative permeabilities (especially in residual gas saturations) and in the dependency of gas and water saturation on capillary pressure can be very large, mainly as a function of the pore network geometry. Only a few cases could be tested here. The effect of a broader range of curve sets should ideally be tested but this is beyond the scope of the present project.

The effect of gas trapped as residual gas may have been overestimated in the simulations here as a consequence of the large cell size. Possibly, migration of CO₂ occurs in stringers of very limited width and thickness. The rock volume penetrated by CO₂ (and thus achieving some CO₂ saturation) is thus probably relatively small, whereas ‘touching’ of a cell in the simulations automatically causes uniform saturation of the whole cell volume. If smaller volumes are saturated in nature than in the simulations, the total volume trapped as residual gas will accordingly be smaller in nature. This effect requires further investigation, e.g. with locally refined grids, but this is beyond the scope of the present study.

Low permeability in Garn

So far, both seismic units (‘Ile’ and ‘Garn’ formations) were treated to have identical reservoir properties. However, if the shallower ‘Garn’ Formation would have lower permeability than the underlying ‘Ile’ Formation, CO₂ migration within it would be slower and CO₂ is expected to reach the sea floor delayed. In addition, CO₂ migrating at the top of the higher permeable ‘Ile’ Formation (below the lower permeable ‘Garn’ Formation) would have a longer lateral distance to the sea floor as compared to the case for migration at the top of the ‘Garn’ Formation (in the base case). In summary, these effects are likely to cause leakage start to be delayed and leakage rates to be smaller than in the base case.

To test this expectation quantitatively, a simulation was carried out in which the ‘Ile’ Formation had the same properties as in the base case, while the ‘Garn’ Formation had a reduced permeability of 20 mD (all other parameters as in base case, incl. base case relative permeability). This simulation predicts that during 2000 years only 1.2% of the total injected CO₂ would leak into the sea (Figure 4.19). CO₂ saturation after 200 and 2000 years in the top of the ‘Garn’ Formation for this case is shown in Figure 4.20.

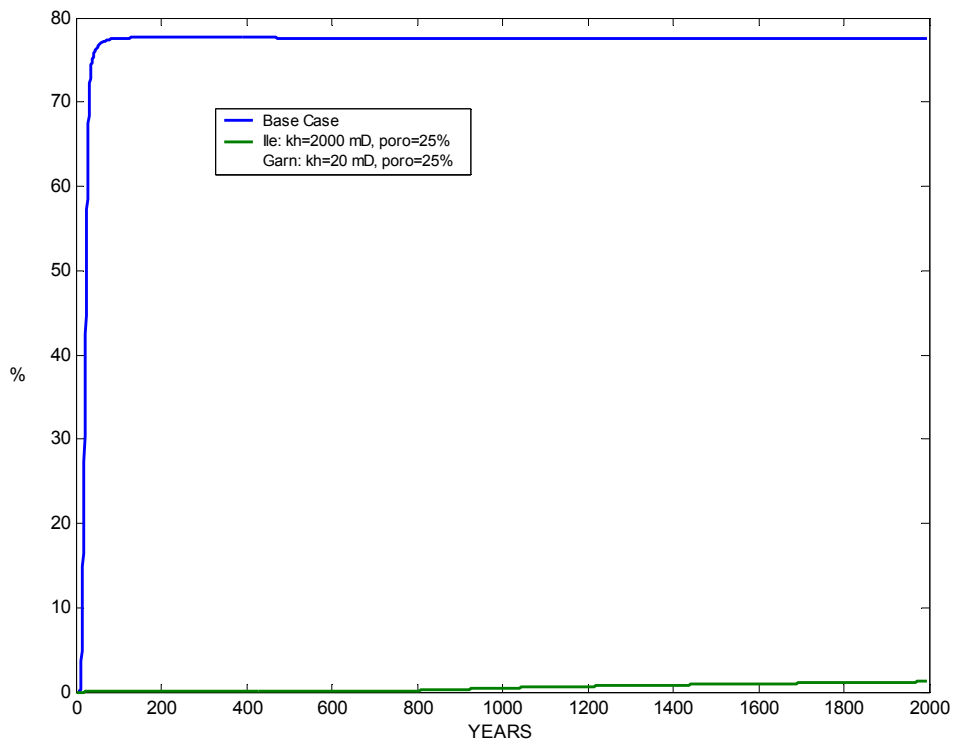
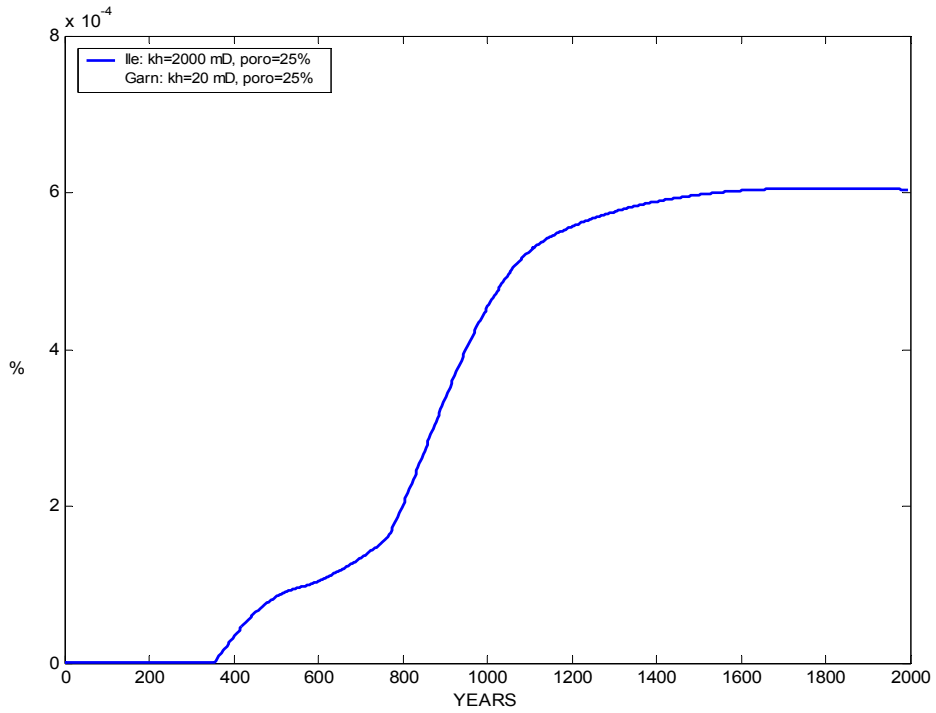


Figure 4.19 Simulated fraction of total injected CO₂ (%) predicted to have leaked from the reservoir; effect of low permeability in the 'Garn' Formation; leaked CO₂ shown as fraction of the total injected amount). Upper: annual rate (note scale, 10⁻⁴ %), lower: cumulative leakage (also of base case for comparison).

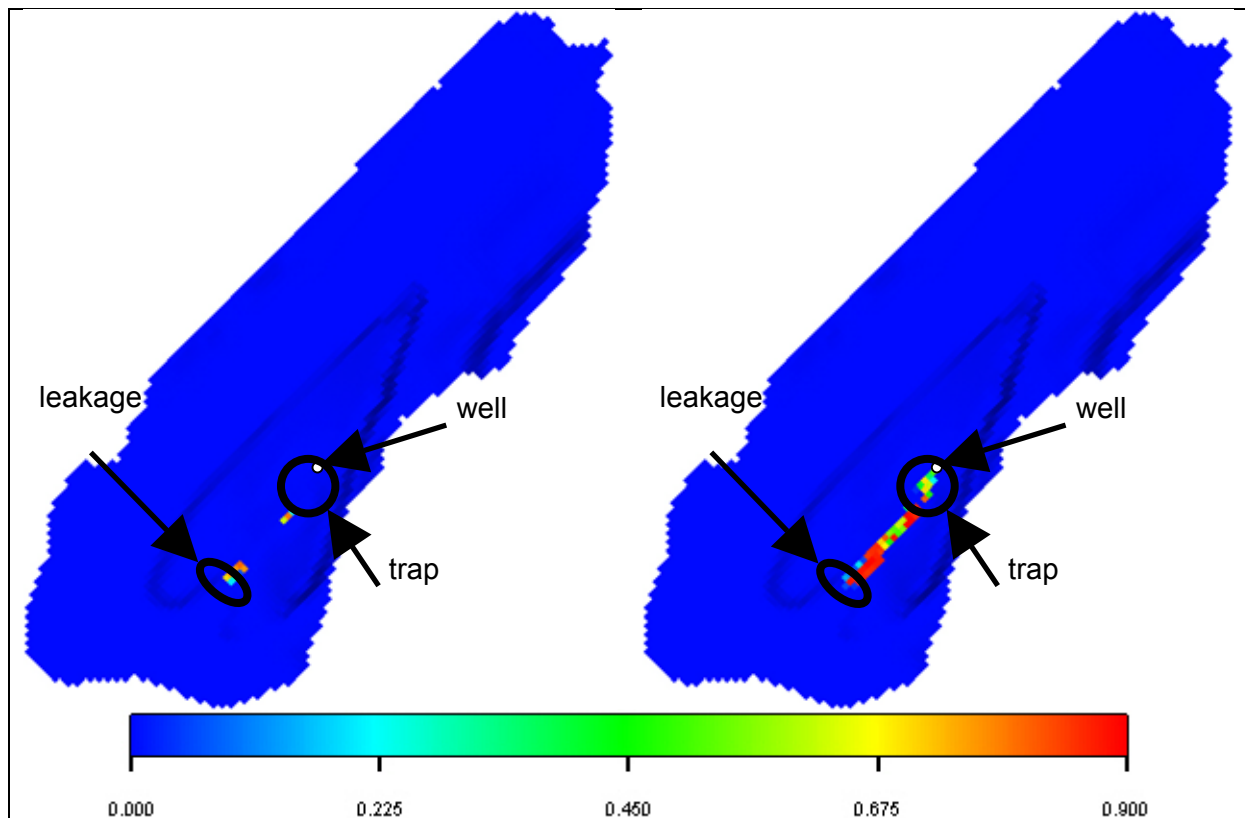


Figure 4.20 *CO₂ saturation at the top of the 'Garn' Formation after 200 years (left) and 2000 years (right); case with reduced permeability of the 'Garn' Formation.*

In an additional case, the alternative relative permeability curves from the previous set of simulations ($S_{gr}=0.10$) and the dependency of gas and water saturation on capillary pressure were employed in addition to the reduced permeability in the 'Garn Formation'. This simulation predicts no leakage during 10 000 years. This is the most favourable case from all simulations carried out.

Injection rate

A further alternative in order to reduce the volume and the fraction of escaping CO₂ is to reduce the quantity of gas that is being injected. The effect of such a strategy was tested by applying a much lower injection rate which was reduced to 10% of that of the base case (that is to 293 000 Sm³ of CO₂ per day). For this case, permeability in both 'Ile' and 'Garn' formations was 20 mD, porosity of 12.5% and k_v/k_h ratio of 0.01. Relative permeability curves used were the same as in the base case and a dependence of fluid saturations on capillary pressure was not applied. This simulation predicts CO₂ not to leak from the reservoir during 5000 years after injection was started. However, this strategy would not fulfil the goal to store all captured CO₂ from a power plant and it would most likely compromise the economy of a CO₂ storage project.

4.5 Simulation results - pressure development

In the presentation of simulation results above, it was assumed that the 'Melke' Formation constitutes a tight seal and can not be entered or traversed by CO₂. However, if injection of

CO₂ into the underlying formations would cause an increase of the pore pressure above the fracture limit, the seal may be fractured and CO₂ could escape almost vertically through the fracture network.

Pore pressure increase would be expected to be especially severe in the case of complete sealing of the reservoir, that is if no formation water could escape from the reservoir. Complete sealing would in the Frohavet case require that the basement, the 'Melke' Formation and the Quaternary would be tight. However, the Quaternary cover of the Frohavet Basin is very thin (mainly less than 10 m in thickness) and partly completely absent. Therefore formation water is likely to be able to leave the reservoir without causing severe overpressure.

The development of the pore pressure at the base of the 'Melke' Formation was monitored and characteristic pressure-time curves are shown in Figure 4.21 for some selected simulations presented above.

Two main other parameters govern the condition for fracturing in addition to the pore pressure: (a) the tensile strength of the rock, and (b) the minimum horizontal stress.

Tensile strength σ_T is a material-specific parameter. For cemented rocks such as the 'Melke' Formation in the Frohavet Basin, tensile strength of the rock matrix is > 0 . However, this assumes that no fractures exist yet. Most likely, fractures (joints) normal to bedding exist already in the 'Melke' Formation. Such fractures may be closed in the subsurface at present, but they reduce the tensile strength of the rock to 0.

For an average water depth above the Frohavet Basin of approximately 320 m, an average thickness of the 'Melke' Formation of 75 m, a water density of 1010 kg/m³, and an estimated bulk density of the 'Melke' Formation of approximately 2500 kg/m³, the minimum horizontal stress is approximately 7.6 MPa (76 bars). Combining this with the tensile strength of 0 MPa, gives an upper limit for the pore pressure increase of 1.36 MPa (13.6 bar).

In none of the simulations carried out in this study, the pressure build-up exceeded the fracturing pressure limit for the 'Melke' Formation (Figure 4.21). The selected cases shown in Figure 4.21 are one with expected low pressure increase (base case) and the two cases with the expected largest pressure increase.

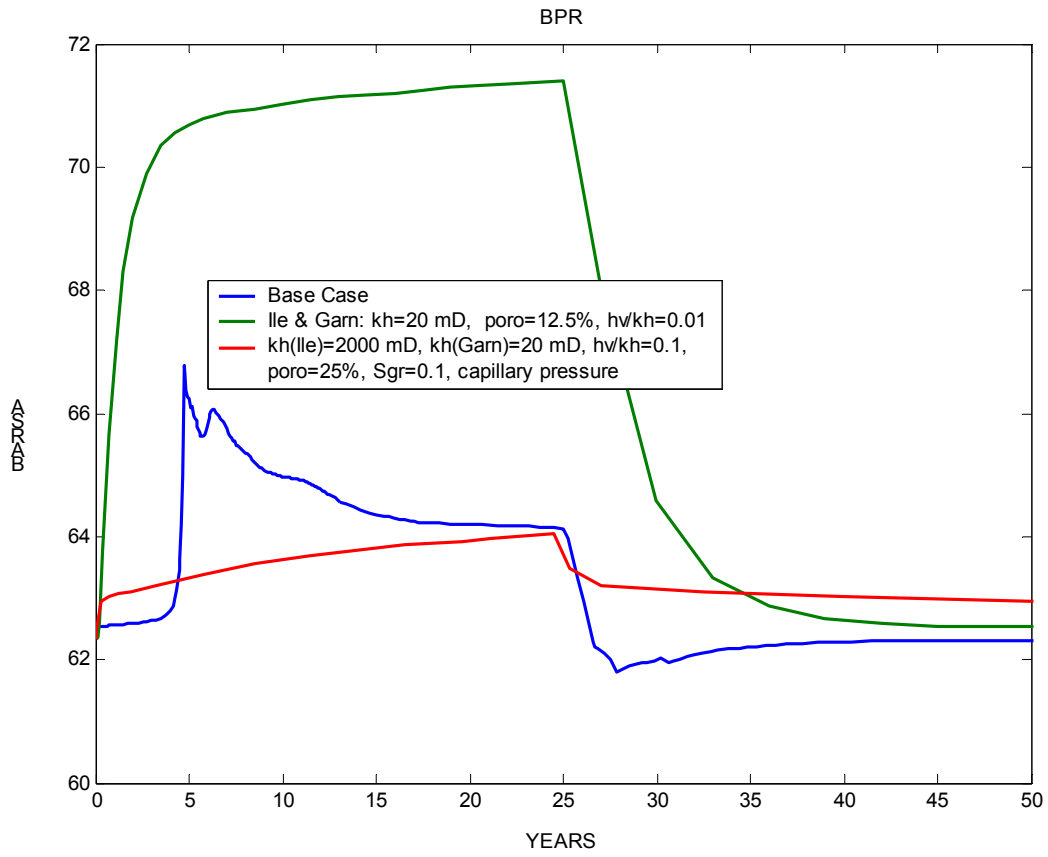


Figure 4.21 Pressure development below the 'Melke' Formation for three selected cases. y-axis: pore pressure in bar.

5. DISCUSSION AND CONCLUSIONS

Summary of observations

Mapping of the Frohavet Basin and the simulation results presented in the previous chapters show some general features:

- The reservoir constitutes an open, south-eastward dipping monocline with a typical migration distance of approx. 4.5 km from potential injection sites to the subcrop of the reservoir formation below the Quaternary or at the sea floor.
- No data about rock properties in the subsurface exist for the Frohavet Basin.
- CO₂ is expected to move upward in the reservoir until it reaches the base of the seal and then to migrate laterally below the seal towards the sea floor.
- In the case of high porosity and high permeability (base case) leakage of CO₂ is predicted to start after a few years and most of the injected CO₂ would have leaked after less than 50 years.
- Lower permeability, lower k_v/k_h ratio, application of a dependency between gas saturation and capillary pressure, high residual gas saturation, and a good injection strategy (well placement and number of wells) are predicted to delay the start of leakage and may reduce the cumulative leaked fraction of CO₂ considerably. Given a favourable combination of these parameters, the onset of leakage may occur only after several centuries after injection start and leakage rates (annual and average) may be in the order of 0.01% of the total injected mass per year. In extremely favourable parameter combinations, no leakage at all may occur.
- There is probably no danger of pressure build-up that would cause fracturing, because the reservoir is not tightly sealed and it has large enough pore volume to accommodate the injected CO₂ volume by water compressibility (an increase in water density).

Difference to the Beitstadfjorden case

The results for the Frohavet Basin are much more promising than those presented earlier for the Beitstadfjorden (Polak et al. 2004). The main differences which make the Frohavet Basin more suitable for long-term storage are:

- Larger pore volume in the reservoir units (almost $52 \cdot 10^9 \text{ m}^3$ here for an assumed porosity of 25%, versus only $1.9 \cdot 10^9 \text{ m}^3$ in the Beitstadfjorden case). This reduces the overpressure generated. Even for the hypothetical case of complete sealing, overpressure in the Frohavet Basin would be much lower than in the Beitstadfjorden.
- Longer migration distance from the optimal injection location to the reservoir subcrop below the Quaternary or the sea floor. This directly delays arrival of CO₂ at the sea floor and indirectly improves dissolution of CO₂ due to a larger surface area in contact with formation water over longer time, which in turn reduces leakage rates and cumulative leaked mass fraction.

Fulfilment of leakage rate criteria

Acceptable leakage rates for reservoirs are presently discussed in the scientific community. A minimum requirement for the performance of underground CO₂ storage sites would be that leakage from them into the atmosphere should not cause worse climatic conditions in the

future than we can expect in the case of direct emission. Recent work indicates that the average storage time should be of the order of a few thousand years or more (Lindeberg 2003) or that annual leakage rates from each single storage site should be less than 0.01 % of the total injected CO₂ (Tore Torp, pers. comm. 2004 on discussions in the IPCC work group on underground CO₂ storage; Hepple & Benson 2002).

Most simulation results for the Frohavet Basin yielded leakage rates that are somewhat or considerably higher than the mentioned acceptable rates. The base case simulation predicted almost complete leakage after only 50 years. However, several simulations employing different reservoir parameters ('worse' in standard hydrocarbon industry terminology, but 'favourable' in the context of CO₂ storage safety) indicate that the Frohavet Basin may have a potential for long-term CO₂ storage if its reservoir formations possess such favourable properties.

Preliminary simulations indicate that there exist very favourable combinations of parameters which could cause very slow and/or very little leakage (possibly no leakage at all).

Principle uncertainties

The simulations contain several uncertainties which are largely due to lacking data on the subsurface. The major uncertainties are:

- The presence, thickness and reservoir properties of the simulated reservoir formations and of their seal.
- The flow properties of the normal fault at the south-eastern margin of the half graben. The injection locations would have to be located deep in the basin, close to the fault, and injected CO₂ may reach the fault. In an ideal case, the fault would be sealing, in a bad case it might constitute a flow path to the surface.
- At a higher geothermal gradient, the density of CO₂ would be lower and the driving force for its migration, buoyancy, be larger. Additionally, its viscosity would be lower, making its flow easier and faster.
- The presence of low-permeable layers within the potential reservoir sequence. Especially, an equivalent to the shaly Not Formation known from Haltenbanken may be present between the 'Ile' and 'Garn' Formations. Its presence may imply that CO₂ injected into the deeper 'Ile' Formation might not reach the 'Garn' Formation. This could have positive and negative consequence; e.g. a larger migration distance to the subcrop or larger pressure increase.

Further alternatives for parameters and curves and their combinations

The simulations presented in this study investigated the influence of some key reservoir parameters on the leakage rate profile. For all these parameters, only a small number of cases could be simulated within the given project frame. For some of them it would be desirable to test a larger variety, for example for the residual gas saturation which may range up to 0.7 (quoted in Holtz 2002).

Hysteretic saturation and flow behaviour was included in the simulations in a simplified manner, treating drainage and imbibition curves as equal, but exhibiting a residual gas saturation. In reality, the imbibition curves would differ from the drainage curves, and the residual gas saturation would strongly depend on the maximum gas saturation achieved

during the drainage process. The ‘residual gas saturation’ used in the present simulations is in fact the maximum residual gas saturation, whereas the real ones would be lower. This effect could be included into more sophisticated simulations.

Residual gas saturation effects may additionally have been overestimated (similarly as in many other recent publications on this topic) due to the simulation set-up, especially due to the cell size. These effects require detailed analysis, for example by simulation of small reservoir volumes with high spatial resolution.

Several of the relevant parameters are not independent of each other, e.g. a more heterogeneous formation with on average low permeability will often have a low k_v/k_h ratio, low relative permeabilities, a strong dependence of gas saturation on capillary pressure (requiring high pressure to achieve high gas saturations) and relatively high residual gas saturations. The systematics in these dependencies and their potential effect on the behaviour of the storage site has not been evaluated yet.

Lack of data

Almost none of the reservoir parameters used in the simulation are based on actual rock data from the subsurface of the Frohavet Basin. The simulations ‘map’ therefore only some of the space of theoretical parameter variations and can only indicate the general potential of the site and if it may be worth to be studied further.

In the simulation presented here, it was assumed that the ‘Melke’ Formation will act as a seal. Its capacity to act as a seal to CO₂ is not known. This requires analyses of rock samples from the formation in the basin.

Summary and proposed way forward

The Frohavet Basin is an open structure, that is, it does not constitute a trap from which CO₂ could not escape without breaching the seal. The suitability of this basin for safe long-term CO₂ storage depends on slow migration of CO₂ towards the surface and the efficacy of processes such as residual gas trapping, trapping in small-scale traps, dissolution of CO₂ into the formation water, and possibly chemical reactions fixing the CO₂ as a compound of minerals.

The Frohavet Basin may be suitable for safe long-term storage of CO₂, given favourable reservoir properties of the potential storage formations. These reservoir properties are at present not known at all due to the complete lack of well data or subsurface samples.

Given industry or public interest for the potential use of this site for long-term CO₂-storage, further appraisal of the basin is proposed here. Such appraisal may be carried out in the following way:

1. Continued mapping of the parameter space, including other scenarios such as sealing between the ‘Ile’ and ‘Garn’ formations and more sophisticated simulations employing full hysteresis, studies of upscaling effects.

If results are positive:

2. Acquisition of subsurface data and samples from one or two wells. These samples should cover the seal and the reservoir interval. Analysis of the data and samples. Revised

reservoir simulations using the new data.

If the well log, samples, and simulations indicate suitable parameters:

3. Acquisition of a 3D seismic survey to determine the subsurface geometry in detail and to derive seismic information about lateral rock heterogeneity (seismic facies). Analysis of the seismic data and revised reservoir simulations.
4. Conclusion about suitability and decision about injection project based on all available data.

6. ACKNOWLEDGEMENTS

NGU and SINTEF would like to thank the Commission of the European Communities (EC-Contract No. ENK-CT-2002-00621), Statoil, Industrikraft Midt-Norge and Klimatek for financial support to this project.

7. REFERENCES

- Bjørlykke, K. 1999: Principal aspects of compaction and fluid flow in mudstones. In: Aplin, A.C., Fleet, A.J., & Macquaker, J.H.S. (eds.): *Muds and Mudstones: Physical and Fluid Flow Properties*. Geological Society, London, Special Publications, 158, pp. 73-78.
- Blystad, P, Brekke, H., Færseth, R.B., Larsen, B.T., Skogseid, J. & Tørudbakken, B. 1995: Structural elements of the Norwegian continental margin. *NPD-Bulletin No 8*, 45 pp.
- Bøe, R. 1991: Structure and seismic stratigraphy of the innermost mid-Norwegian continental shelf: and example from the Frohavet area. *Marine and Petroleum Geology* 8, 140-151.
- Bøe, R. & Bjerkli, K. 1989: Mesozoic sedimentary rock in Edøyfjorden and Beitstadfjorden, Central Norway: Implications for the structural history of the Møre-Trøndelag fault zone. *Marine Geology* 87, 287-299.
- Bøe, R., Magnus, C., Osmundsen, P.T. & Rindstad, B.I. 2002: CO₂ point sources and subsurface storage capacities for CO₂ in aquifers in Norway. NGU Report 2002.010, 132 pp.
- Corey, A.T. 1976: *Mechanics of heterogeneous fluids in porous media*. Water Resources Publications.
- Ehrenberg, S.N. 1990: Relationship between diagenesis and reservoir quality in sandstones of the Garn Formation, Haltenbanken, mid-Norwegian continental shelf. *Bulletin American Association of Petroleum Geologists* 74, 1538-1558.
- Enick, R.M. & Klara, S.M. 1990: CO₂ solubility in water and brine under reservoir conditions. *Chem. Eng. Comm.*, 90, 23-33.
- Ennis-King, J., Gibson-Poole, C.M., Lang, S.C. & Paterson, L. (2002): Long-term numerical simulation of geological storage of CO₂ in the Petrel Sub-basin, North-West Australia. In: Gale, J. & Kaya, Y. (eds.): *Greenhouse Gas Control Technologies (Proceedings of the 6th International Conference on Greenhouse Gas Control Technologies, Kyoto, Japan, October 2002)*, Addendum, 11-16, Pergamon, Oxford (UK).
- Gabrielsen, R.H., Odinsen, T., & Grunnaleite, I. 1999: Structuring of the northern Viking Graben and the Møre Basin; the influence of basement structural grain, and the particular role of the Møre-Trøndelag Fault Complex. *Marine and Petroleum Geology* 16, 443-465.
- Gran, I.Ø. 1990: En diagnetisk studie av noen utvalgte midt-Jurassiske slam- og sansteinsprøver fra Frohavetbassenget. Unpublished Masters Thesis, NTNU, Trondheim, 151 p.
- Hepple, R.P. & Benson, S.M. 2002: Implications of surface seepage on the effectiveness of geological storage of carbon dioxide as a climate change mitigation strategy. In: Gale, J. & Kaya, Y. (eds.): *Greenhouse Gas Control Technologies (Proceedings of the 6th International Conference on Greenhouse Gas Control Technologies, Kyoto, Japan, October 2002)*, vol 1, pp. 261 – 266, Pergamon, Oxford (UK).

- Holtz, M.H., Residual gas saturation to aquifer influx: a calculation method for 3-D computer reservoir model construction. SPE Paper 75502. SPE Gas technology Symposium, Calgary, Alberta, Canada, 30. April – 2. May 2002.
- Johansen, M., Poulsen, H., Skjæran, H., Straume, T. & Thorsplass, J.O. 1988: Froanbassengets dannelse og Jurassiske sedimenter. Internal project report NTNU, 104 pp.
- Kelly, S.R.A. 1988: Middle Jurassic marine macrofauna from erratics in Trøndelag, Norway. Unpublished Internal NTNU report, 33 p.
- Koch, J.-O. & Heum, O.R. 1995: Exploration trends of the Halten Terrace. In: Hanslien, S. (ed), Petroleum Exploration and Exploitation in Norway, NPF Special Publication 4, 235-251.
- Lindeberg, E. & Bergmo, P. 2003: The long-term fate of CO₂ injected into an aquifer. In: Gale, J. & Kaya, Y. (eds.): Greenhouse Gas Control Technologies (Proceedings of the 6th International Conference on Greenhouse Gas Control Technologies, Kyoto, Japan, october 2002), vol 1, pp. 489 – 494, Pergamon, Oxford (UK).
- Lindeberg, E. 2003: The quality of a CO₂ repository: What is the sufficient retention time of CO₂ stored underground? In: Gale, J. & Kaya, Y. (eds.): Greenhouse Gas Control Technologies (Proceedings of the 6th International Conference on Greenhouse Gas Control Technologies, Kyoto, Japan, october 2002), vol 1, pp. 255 – 260, Pergamon, Oxford (UK).
- Lindeberg, E., van der Meer, B., Moen, A., Wessel-Berg, D. & Ghaderi, A. 2000: Saline Aquifer CO₂ Storage (SACS): Task 2: Fluid and core properties and reservoir simulation. Report period: 01/11/98 – 31/12/99, SINTEF Petroleum Research, Report no. 54.5148.00/02/00
- Mørk, M.B., Johnsen, S.O. & Torsæter, O. 2003: Porosity and permeability examination of Jurassic samples from Froøyane. Unpublished NTNU report, 5 pp.
- Nordhagen, R. 1921: Fossilførende blokker fra Juratiden på Froøyene utenfor Trondheimsfjorden. *Naturen* 45, 110-115.
- Oftedahl, C. 1975: Middle Jurassic graben tectonics in Mid-Norway. Proceedings of the Jurassic northern North Sea Symposium, Stavanger. Norwegian Petroleum Society, Oslo, 1-13.
- Polak, S., Lundin, E., Bøe, R., Lindeberg, E., Olesen, O. & Zweigel, P.: Storage potential for CO₂ in the Beitstadfjord Basin, Mid-Norway. NGU report 2004.036, SINTEF report 54.5272.00/01/04. Norges Geologiske Undersøkelse, Trondheim.
- Riis, F. 1996: Quantification of Cenozoic vertical movements of Scandinavia by correlation of morphological surfaces with offshore data. *Global and Planetary Change* 12, 331-357.
- Rise, L., Haugane, E. & Johnsen, S.O. 1989: Blokkleting på Froøyene 1987. IKU Report 24.1511.00/01/89, 23 pp.
- Sommaruga, A., & Bøe, R. 2003: Geometry and subcrop maps of shallow Jurassic basins along the Mid-Norway coast. *Marine and Petroleum Geology* 19, 1029-1042.

- Twiss, R.J. & Moore, E.M. 1992: Structural geology. 532 pp., W.H., Freeman & Co, New York (US).
- van Genuchten, M. Th. 1980: A closed-form equation for predicting the hydraulic conductivity of unsaturated soils. Soil Sci. Soc. Am. J., 44, 892-898.
- Weisz, G. 1992: An investigation of Jurassic coals from Haltenbanken and Beitstadsfjorden. A comparison of composition and maturity. Diploma thesis at the Department of Geology and Mineral Resources, Technical University of Trondheim (NTNU), Trondheim, Norway, 79 pp.